



HAL
open science

Palaeoenvironmental changes in the southwestern Mediterranean (ODP site 976, Alboran sea) during the MIS 12/11 transition and the MIS 11 interglacial and implications for hominin populations

Dael Sassoon, Vincent Lebreton, Nathalie Combourieu-Nebout, Odile Peyron, Marie-Hélène Moncel

► To cite this version:

Dael Sassoon, Vincent Lebreton, Nathalie Combourieu-Nebout, Odile Peyron, Marie-Hélène Moncel. Palaeoenvironmental changes in the southwestern Mediterranean (ODP site 976, Alboran sea) during the MIS 12/11 transition and the MIS 11 interglacial and implications for hominin populations. *Quaternary Science Reviews*, 2023, 304, pp.108010. 10.1016/j.quascirev.2023.108010 . hal-04000017

HAL Id: hal-04000017

<https://hal.science/hal-04000017>

Submitted on 12 Oct 2023

HAL is a multi-disciplinary open access archive for the deposit and dissemination of scientific research documents, whether they are published or not. The documents may come from teaching and research institutions in France or abroad, or from public or private research centers.

L'archive ouverte pluridisciplinaire **HAL**, est destinée au dépôt et à la diffusion de documents scientifiques de niveau recherche, publiés ou non, émanant des établissements d'enseignement et de recherche français ou étrangers, des laboratoires publics ou privés.

1 **Title:** Palaeoenvironmental Changes in the Southwestern Mediterranean (ODP Site 976,
2 Alboran Sea) During the MIS 12/11 Transition and the MIS 11 Interglacial and Implications
3 for Hominin Populations

4

5 **Authors:** Dael SASSOON^{1*}, Vincent LEBRETON¹, Nathalie COMBOURIEU-NEBOUT¹, Odile
6 PEYRON², Marie-Hélène MONCEL¹

7

8 **Affiliations:**

9 1: Muséum national d'Histoire naturelle, UMR 7194 Histoire Naturelle de l'Homme
10 Préhistorique, Paris

11 2: Institut des Sciences de l'Évolution de Montpellier, UMR 5554, Université de Montpellier

12

13 * *corresponding author*

14 **Palaeoenvironmental Changes in the Southwestern Mediterranean (ODP Site 976, Alboran**
15 **Sea) During the MIS 12/11 Transition and the MIS 11 Interglacial and Implications for**
16 **Hominin Populations**

17
18 **Dael SASSOON^{1*}, Vincent LEBRETON¹, Nathalie COMBOURIEU-NEBOUT¹, Odile PEYRON²,**
19 **Marie-Hélène MONCEL¹**

20 ¹*Muséum national d'Histoire naturelle, UMR 7194 Histoire Naturelle de l'Homme Préhistorique, Paris*

21 ²*Institut des Sciences de l'Évolution de Montpellier, UMR 5554, Université de Montpellier*

22
23 **Abstract**

24 The transition from the Marine Isotope Stage (MIS) 12 glacial (ca. 478–424 ka BP) to the MIS
25 11 interglacial (ca. 424–365 ka BP) is one of the most remarkable climatic shifts of the Middle
26 Pleistocene and is regarded as a phase of major behavioural innovation for hominins.
27 However, many of the available pollen records for this period are of low resolution or
28 fragmented, limiting our understanding of millennial-scale climatic variability. We present a
29 high-temporal resolution pollen record that encompasses the period between MIS 12 and
30 MIS 10 (434–356 ka BP), recovered from the Ocean Drilling Program (ODP) Site 976 in the
31 Alboran Sea. This study aims to provide new insights into the response of vegetation during
32 the transition and to highlight patterns of climatic variability during MIS 11.

33 The ODP Site 976 pollen record shows the shift from glacial to interglacial at 426 ka BP,
34 highlighted by the transition from *Pinus*, herbaceous and steppic taxa to temperate and
35 Mediterranean taxa. A climatic optimum for temperate and Mediterranean taxa is identified
36 around 426–400 ka BP, equivalent to substage MIS 11c and synchronous with the maxima in
37 SSTs, greenhouse gas concentrations and insolation. A phase with increased *Pinus* and *Cedrus*
38 indicates the return to colder and more arid conditions during substage MIS 11b (400–390 ka
39 BP). Substage MIS 11a (390–367 ka BP) is marked by a period of short-term warming followed
40 by gradual cooling, until the return of glacial conditions during MIS 10. Forest contractions
41 have been linked with high- and moderate-intensity climate events also observed in other
42 pollen records and proxies from the Mediterranean and North Atlantic.

43 Our results confirm the intense shift during the MIS 12/11 transition and show that this
44 region is sensitive to millennial-scale climatic variation during MIS 11. The forest contractions
45 observed in our record during events of millennial-scale variability appear to be less intense
46 than in the central and eastern Mediterranean. This suggests that the southwestern
47 Mediterranean may have been less variable during periods of climatic deterioration, thereby
48 representing a possible ecological niche for vegetation. This may have provided a source of
49 subsistence for hominins during harsher conditions, thus contributing to their demographic
50 expansion and technological innovations.

51
52 **Keywords:** Southwestern Mediterranean; Middle Pleistocene; Marine record; Pollen;
53 Vegetation dynamics; Long-term vegetation change; Climate change; Millennial-scale climate
54 variability

55
56 **1. Introduction**

57 The transition from the extensive glaciation of MIS (Marine Isotope Stage) 12 to the
58 remarkably long and warm MIS 11 interglacial is regarded as one of the most extreme climatic
59 shifts over the last 900 ka (Chaisson *et al.*, 2002; Tzedakis *et al.*, 2009; Sánchez Goñi *et al.*,
60 2016; Marino *et al.*, 2018). This shift, occurring during Termination V (TV), stands out in the

61 Middle Pleistocene due to the exceptional increase in sea levels and greenhouse gas
62 concentrations from MIS 12 to MIS 11 despite minimal astronomical forcing—what Berger
63 and Wefer (2003) defined as the “Stage-11 Paradox”. In marine and terrestrial records, the
64 MIS 12 glacial (ca. 478–424 ka BP) is often deemed as one of the most severe glacial periods
65 of the Pleistocene, during which the global ice volume exceeded that of the Last Glacial
66 Maximum (LGM) and the European ice sheet reached its maximum of the last 1.2 Ma (Olson
67 and Hearty, 2009; Toucanne *et al.*, 2009; Koutsodendris *et al.*, 2019). Pollen records
68 from Tenaghi Philippon (e.g. Tzedakis *et al.*, 2006; Pross *et al.*, 2015) and Lake Ohrid (Sadori
69 *et al.*, 2016; Kousis *et al.*, 2018) show that this period was characterised by severe reductions
70 in tree populations associated with a prevalence of cold conditions. In contrast, especially
71 warm and humid conditions prevailed during MIS 11 (ca. 424–365 ka BP) even in the higher
72 latitudes of the Northern Hemisphere (Kousis *et al.*, 2018) over a period longer than any other
73 interglacial of the Mid- to Late Pleistocene (Marino *et al.*, 2018). The climatic optimum during
74 substage MIS 11c has been widely recognised as a long, warm and relatively stable period of
75 the interglacial in both marine and terrestrial records across the Mediterranean, showing that
76 these conditions prevailed across the wider region (e.g. Oliveira *et al.*, 2016; Kousis *et al.*, 2018;
77 Azibeiro *et al.*, 2021). Such a long-lasting interglacial period after the harsh glacial conditions
78 of MIS 12 favoured the development of temperate vegetation across Europe and in turn led
79 to the demographic expansion of hominin populations (Berger and Loutre, 2003; Raymo *et al.*
80 *et al.*, 2012; Oliveira *et al.*, 2016; Moncel *et al.*, 2018).

81 Indeed, from a hominin evolution point of view, the MIS 12/11 transition represents a
82 significant threshold period. Genetic data and anthropological analyses have recently shown
83 that European Neanderthal features emerged in the population between 600 and 400 ka
84 (Hublin, 2009) and that climatic amelioration after the MIS 12 glaciation led to a phase of
85 major innovation for hominins. Archaeological records for this period show evidence of
86 increased occupations, new subsistence behaviours and technical innovations (e.g. core
87 technologies, increase in light-duty tools), and an early regionalization of traditions (Moncel
88 *et al.*, 2016; Blain *et al.*, 2021). Investigating vegetation changes during this period is key to
89 improving our understanding of the impacts of climate on biomass availability for large
90 herbivores, the mobility of human groups and demographic changes.

91 Furthermore, in recent years MIS 11 has received a noticeable amount of attention as it
92 is regarded as one of the best analogues to the Holocene (MIS 1) (Loutre and Berger, 2003;
93 Candy *et al.*, 2014). Both interglacials, MIS 11 and MIS 1, are characterised by high sea levels,
94 intense warmth, low astronomical forcing—in particular low precession—and elevated
95 atmospheric CO₂ concentrations (McManus *et al.*, 2003; Desprat *et al.*, 2005; Hes *et al.*, 2022).
96 This makes MIS 11 an important period for investigating climatic variability and its impacts on
97 vegetation and hominin populations during conditions similar to those of the current
98 interglacial.

99 Although the MIS 12/11 transition has been previously studied across the Mediterranean
100 (Fig. 1, Tab. 1) through the use of terrestrial (pollen) and marine climatic indicators (planktic
101 foraminifera and oxygen isotopes), many of the available records are of relatively low-
102 temporal resolution and/or fragmented (e.g. Desprat *et al.*, 2005; Tzedakis *et al.*, 2009). Thus,
103 our understanding of short-term vegetation change and millennial-scale climatic variability is
104 still limited. Important advances have been recently made with records from the Iberian
105 margin (Desprat *et al.*, 2005, 2007; Oliveira *et al.*, 2016, Hes *et al.*, 2022) and new studies have
106 attempted to increase the resolution of existing records, such as Lake Ohrid (Kousis *et al.*,
107 2018) and Tenaghi Philippon (Ardenghi *et al.*, 2019). These studies have shown the

108 importance of long records with a high-temporal resolution to better understand the
 109 amplitude of centennial-scale changes in temperature, precipitation, and the length of cold
 110 episodes. However, more research is required to understand the responses of vegetation to
 111 climate and the changes in temperature and precipitation during this transition across the
 112 Mediterranean region, especially in the southwestern area where only few and fragmentary
 113 terrestrial records are available (e.g. Atapuerca; Rodríguez *et al.*, 2011).

114 In this study, we present a high-temporal resolution pollen record recovered from the
 115 ODP Site 976 in the Alboran Sea that encompasses a long timeframe from MIS 12 to MIS 10
 116 (434–356 ka BP). The continuous, high-resolution pollen data generated in this study allowed
 117 the study of millennial-scale vegetation changes and comparisons with other high-resolution
 118 pollen and climatic records in the Mediterranean. This study aims to: (1) provide a new high-
 119 resolution pollen record encompassing the MIS 12/11 transition; (2) reconstruct regional
 120 landscape-scale changes in vegetation; (3) highlight patterns of climate variability in the
 121 Mediterranean region; and (4) discuss hominin subsistence in this context.

122

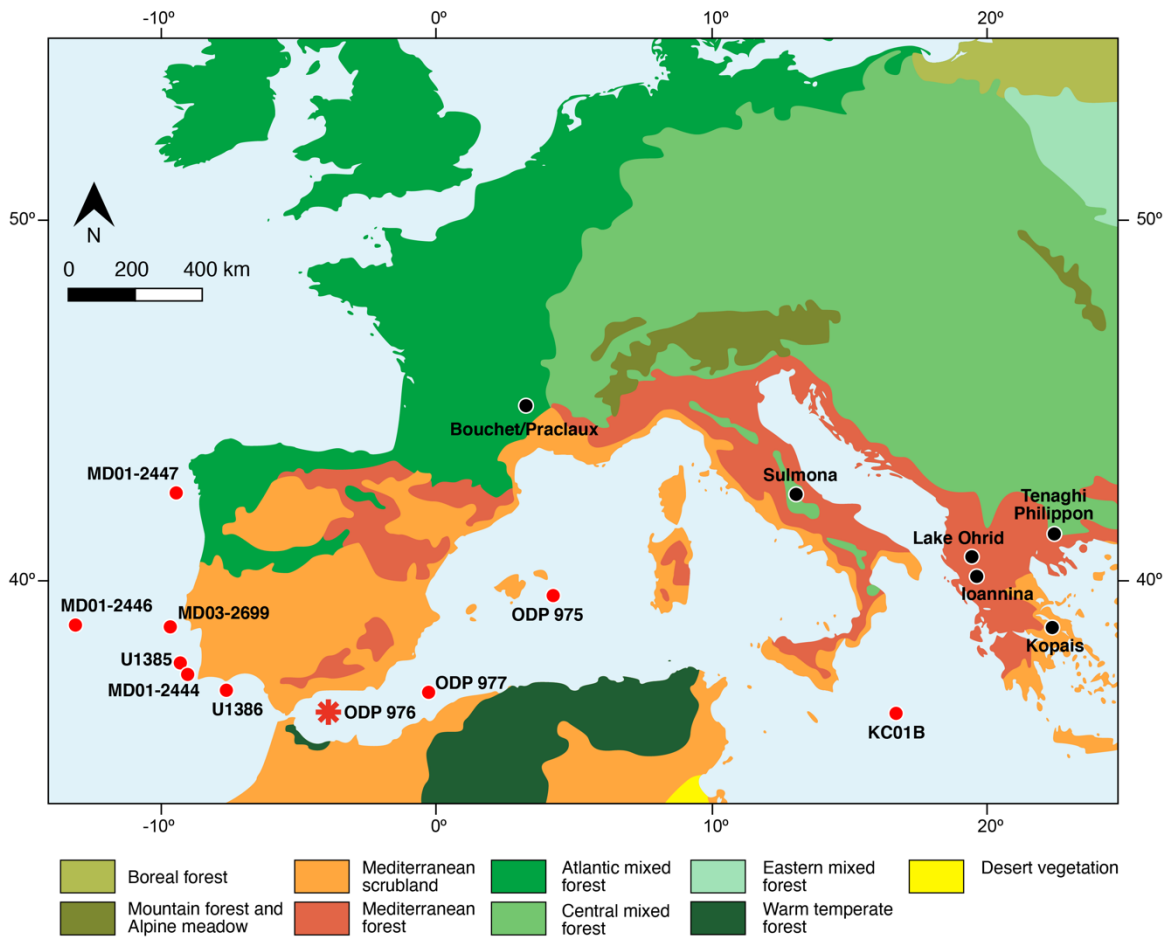


Figure 1 – Map showing the modern vegetation distribution (modified from Sánchez Goñi, 2022). The location of ODP Site 976 is indicated with a red star along with other marine (red dots) and terrestrial (black dots) proxy records covering MIS 12 and 11 discussed in the text. For more information about the sites and proxies used see Table 1.

123

Table 1 – Terrestrial and marine records from the Mediterranean covering MIS 12 and 11.

Site name	Site type	Lat (°N)	Long (°W)	Elevation (m)	Period (ka BP)	MIS stages	Record type	References
-----------	-----------	----------	-----------	---------------	----------------	------------	-------------	------------

Ioannina	Terrestrial	39.4	20.51	470 asl	500-0	13-1	Pollen	Tzedakis, 1993, 1994; Tzedakis <i>et al.</i> , 1997, 2001
IODP U1385	Marine	37.57	-10,12	2578 bsl	440-365	12a-10c	Pollen, alkenones	Oliveira <i>et al.</i> , 2016
IODP U1386	Marine	36.83	-7,76	561 bsl	433-404	12a-11d	Pollen	Hes <i>et al.</i> , 2022
KC01B	Marine	36.15	17.44	3643 bsl	1200-0	36-1	Foraminifera, $\delta^{18}\text{O}$	Lourens, 2004
					464-419	12c-11c	Foraminifera, $\delta^{18}\text{O}$	Azibeiro <i>et al.</i> , 2021
Kopais	Terrestrial	38.37	23.13	95 asl	500-0	13-1	Pollen	Okuda <i>et al.</i> , 2001
Lac du Bouchet	Terrestrial	44.55	3.47	1200 asl	450-0	12-0	Pollen	Reille and De Beaulieu, 1995
Lac du Praclaux	Terrestrial	44.49	3.5	1100 asl	450-1	12-1	Pollen	Reille and de Beaulieu, 1990 ; Reille and de Beaulieu, 1995 ; Reille <i>et al.</i> , 1998
Lake Ohrid	Terrestrial	41.02	20.42	1514 asl	500-0	13-1	Pollen, foraminifera, $\delta^{18}\text{O}$	Sadori <i>et al.</i> , 2016; Wagner <i>et al.</i> , 2019
					465-430	12a-10c	Pollen, tephra	Kousis <i>et al.</i> , 2018
MD01-2444	Marine	37.33	10.08	2637 bsl	430-0	12-0	Foraminifera, $\delta^{18}\text{O}$, alkenone	Martrat <i>et al.</i> , 2007
MD01-2446	Marine	39.03	12.37	3570 bsl	545-300	14-9	Foraminifera, $\delta^{18}\text{O}$	Voelker <i>et al.</i> , 2010
					550-290	14-8	Foraminifera, calcareous nanofossil, $\delta^{18}\text{O}$	Marino <i>et al.</i> , 2014
MD01-2447	Marine	42.15	-9.67	2080 bsl	426-394	12-11	Pollen, foraminifera, $\delta^{18}\text{O}$	Desprat <i>et al.</i> , 2005, 2007
MD03-2699	Marine	39.02	10.39	1865 bsl	580-300	15-9	Alkenones	Rodrigues <i>et al.</i> , 2011
ODP975	Marine	38.53	4.3	2415 bsl	1200-0	36-0	Foraminifera, $\delta^{18}\text{O}$	Pierre <i>et al.</i> , 1999; Lourens, 2004
					650-250	16-8	Foraminifera, $\delta^{18}\text{O}$	Girone <i>et al.</i> , 2013
ODP976	Marine	36.12	4.18	1108 bsl	434-357	12a-10c	Pollen	This study
ODP977	Marine	36.01	1.57	1984 bsl	540-300	13c-9a	Foraminifera, calcareous nanofossil, $\delta^{18}\text{O}$	Marino <i>et al.</i> , 2018; Azibeiro <i>et al.</i> , 2021
Sulmona basin	Terrestrial	-	-	360-2000 asl	500-410	13-11	Speleothems, lithology, XRF, CaCO ₃ content, carbonate $\delta^{18}\text{O}$ and $\delta^{13}\text{C}$	Regattieri <i>et al.</i> , 2016
Tenaghi Philippon	Terrestrial	41.10	24.2	40 asl	440-330	12-10	Pollen, alkenone, brGDGTs, leaf wax, levoglucosan	Ardenghi <i>et al.</i> , 2019
					1400-0	42-1	Pollen	Tzedakis <i>et al.</i> , 2006
					460-335	12-10	Cryptotephra	Vakhrameeva <i>et al.</i> , 2018

124

125

126

2. Regional setting

127

This study used sections of the long marine sequence recovered during Leg 161 of the Ocean Drilling Program (ODP) (Shipboard Scientific Party, 1996) from ODP Site 976 in the Western Alboran Sea (Fig. 2; 36°12.3'N 4°18.8'W), located about 110 km from the Strait of Gibraltar at 1108 m water depth (Combourieu-Nebout *et al.*, 1999, 2009; Gonzalez-Donoso *et al.*, 2000).

128

129

130

131 The Alboran Sea, a narrow extensional basin measuring 150 km wide and 350 km in
132 length (Alonso *et al.*, 1999) is a transitional area between the Mediterranean Sea and the
133 Atlantic Ocean (Bulian *et al.*, 2022), and represents the westernmost side of the
134 Mediterranean, bordered by Spain to the north and Morocco to the south.

135 Circulation in the Alboran Sea is strong, mainly due to the water exchange at the Strait of
136 Gibraltar between the inflow of low-salinity waters from the Atlantic and the outflow of high-
137 salinity Mediterranean waters, which results in two anti-cyclonic gyres known as the Western
138 and Eastern Alboran Gyres (WAG and EAG, respectively) (Bulian *et al.*, 2022). ODP976 is
139 located near the centre of the WAG (Fig. 2).

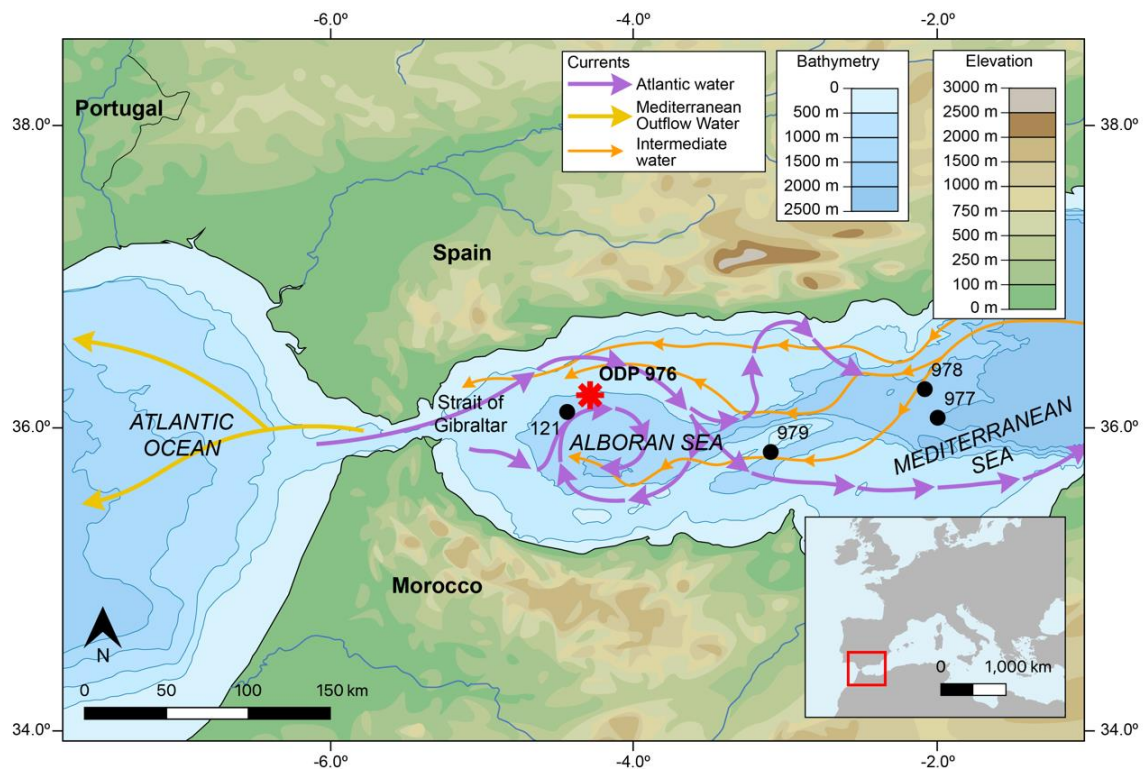


Figure 2 – Map showing the location of ODP Site 976 and the present-day surface and water circulation in the Alboran Sea (modified from Combourieu-Nebout *et al.*, 1999). Other ODP sites are marked with black dots.

140 The climate in this region is Mediterranean and strongly influenced by the Southern
141 Azores cyclone in summer which results in long, dry summers and mild, rainy winters
142 (Combourieu-Nebout *et al.*, 1999, 2009). Mean temperatures of the coldest months range
143 between 10°C near the coast and -7°C at altitudes above 2000 m, while mean temperatures
144 of the warmest months usually exceed 25°C (Garcia-Gorriz and Garcia-Sanchez, 2007; Parada
145 and Canton, 1998); annual precipitation ranges between 400 and 1400 mm (Combourieu-
146 Nebout *et al.*, 2009).

147 The landscape is enclosed by the mountains of the Moroccan Rif and Betic Cordillera,
148 leading to an altitudinal range of vegetation (Quézel and Medail, 2003). Steppe vegetation
149 with *Lygeum*, *Artemisia* and a Mediterranean group of taxa including *Olea*, *Phillyrea*, *Pistacia*,
150 and *Quercus ilex* dominates the coast. This assemblage is replaced by a humid-temperate oak
151 forest with *Quercus deciduous* and Ericaceae at mid-altitudes, and finally by cold-temperate
152 coniferous forests with *Pinus* and *Abies* at higher elevations. Currently, *Cedrus* is typically
153 found in the higher elevations of Morocco (Ozenda, 1975; Rivas Martínez, 1982; Barbero *et*
154 *al.*, 1981; Benabid, 1982).

155 The location of ODP976 was chosen because previous studies have shown that the
156 Western Alboran Sea is particularly sensitive to centennial and millennial climate change due
157 to its unique exposure to polar tropical and Atlantic influences (Alonso *et al.*, 1999;
158 Combourieu-Nebout *et al.*, 1999, 2002, 2009; Bulian *et al.*, 2022). It has also been recently
159 the focus of studies on planktonic foraminifera to investigate MIS 12 and 11 by Marino *et al.*
160 (2018) and Azibeiro *et al.* (2021), showing the ability of this location to record climatic
161 variability during this particular period.

162

163 **3. Material and Methods**

164

165 **3.1 Chronology**

166 **3.1.1 Age model**

167 The chronology for this study has been adopted
168 from von Grafenstein *et al.* (1999), who
169 correlated the biostratigraphic marker events in
170 the study by de Kaenel *et al.* (1999) on ODP976
171 (i.e. changes in the planktonic foraminifera
172 *Globigerina bulloides*) with the benthic oxygen
173 isotope record of Site 659. The ages presented
174 here are in calendar ka (cal ka), consistent with
175 the model developed by von Grafenstein (Fig. 3)
176 and other studies that have adopted this
177 chronology for the ODP976 core (e.g.
178 Combourieu-Nebout *et al.*, 2009). Age
179 interpolation of the record has a maximum age of
180 433.868 ka BP at 118.8 m and a minimum age of
181 356.456 ka BP at 98.85 m. Interpolation was achieved with the *interpol* function of *tidypalaeo*
182 on R.

183

184 **3.1.2 MIS subdivision**

185 MIS 11 is traditionally divided into three substages: a, b and c (Hrynowiecka *et al.*, 2019). This
186 subdivision has been adopted by most palynological studies in the Mediterranean (e.g.
187 Oliveira *et al.*, 2016; Kousis *et al.*, 2018; Ardenghi *et al.*, 2019). Recent palaeoclimatic studies
188 on MIS 11 in the Northern Hemisphere have introduced two additional substages at the base
189 of MIS 11 (11d and 11e) based on minor changes in isotopic data (Railsback *et al.*, 2015;
190 Hrynowiecka *et al.*, 2019). This distinction seems to be highly dependent on the geographical
191 location of the records, their temporal resolution and the proxies used, and so far only few
192 records have applied a five-substage subdivision—among pollen studies, this partition has
193 been used in the North Atlantic off the coast of Iberia, but not in the Mediterranean.
194 Therefore, we followed the more widely applied nomenclature for MIS 11, defining the base
195 of the interglacial as MIS 11c.

196

197 **3.2 Pollen analysis**

198 A total of 141 samples were selected from Holes 976 B13, B12 and C12 of the ODP Site 976
199 marine core (representing the depths 98–119 m, dated between MIS 12 and MIS 10), at an
200 average resolution of 10 cm with occasional higher resolution in specific areas of interest.
201 Samples were dried and 5 g of sediments were treated following standard methods (Faegri

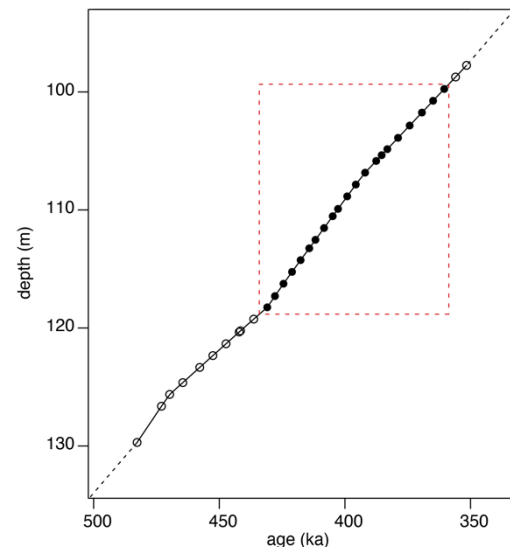


Figure 3 – Age model by von Grafenstein *et al.* (1999). Black dots within the red dotted square highlight the chronological interval adopted for this study.

202 and Iversen, 1989) under 10% HCL, 40% HF and 20% HCL and sieved with a 10 µm sieve
 203 (Combourieu-Nebout *et al.*, 2009). Acetolysis was avoided to preserve dinoflagellates. Two
 204 *Lycopodium* tablets (batch number: 1031) were added to calculate absolute pollen
 205 concentrations (pollen grains per unit of sediment volume).

206 A minimum of 150 grains of total land pollen (TLP) were counted for each sample,
 207 excluding *Pinus* because of their natural overrepresentation in European biomes and marine
 208 records (Fletcher and Sánchez Goñi, 2008; Sánchez Goñi *et al.*, 2009; Sadori *et al.*, 2016), as
 209 well as aquatics (e.g. *Cyperaceae* and *Typha/Sparganium*) and fungal/algal spores (e.g.
 210 Pteridophyta). Ecological groups were based on modern climate-vegetation associations and
 211 follow the main groups defined by Suc (1984). Despite having subtropical and temperate
 212 affinities respectively, pollen grains of *Carya* and *Euonymus* were found at very low levels
 213 (<1.3%) and therefore these taxa were included within the Ubiquist group. A target of 20
 214 morphotypes was chosen to ensure an appropriate representation of vegetation
 215 composition.

216 The percentage pollen diagrams were developed using the *Rioja* package in the software
 217 *R* (Juggins, 2020). Taxa were divided into ecological groups representative of specific climatic
 218 conditions (Tab. 2).
 219

Table 2 – Taxa included in each ecological group

Ecological group	Taxa
Riparian	<i>Betula, Alnus, Pterocarya, Fraxinus, Ilex, Salix</i>
Montane	<i>Abies, Picea, Cedrus, Tsuga</i>
Temperate	<i>Acer, Hedera, Carpinus betulus, Corylus, Quercus deciduous, Fagus, Castanea, Juglans, Tilia, Ulmus, Fraxinus ornus</i> type
Mediterranean	<i>Pistacia, Buxus, Quercus ilex, Quercus suber, Olea, Phillyrea, Ostrya carpinifolia, Cistus, Arbutus unedo</i>
Herbaceous	Apiaceae undiff., Asteroidae, Cichorioideae, <i>Helianthemum</i> , Convolvulaceae undiff., Ericaceae undiff., <i>Erica arborea</i> type, Lamiaceae undiff., Liliaceae undiff., <i>Asphodelus</i> , Plantaginaceae undiff., <i>Plantago, Plantago lanceolata</i> , Celastraceae undiff.
Pioneer	Cupressaceae undiff., <i>Juniperus, Centaurea, Centaurea scabiosa, Centaurea cyanus</i>
Steppic	<i>Artemisia</i> , Chenopodiaceae undiff., <i>Ephedra distachya, Ephedra fragilis</i> , Poaceae undiff., <i>Paronychia/Herniaria, Lygeum</i>
Ubiquists	Brassicaceae undiff., Gentianaceae, Campanulaceae undiff., Caryophyllaceae undiff., Cistaceae undiff., Dipsacaceae undiff., <i>Scabiosa, Knautia</i> , Euphorbiaceae undiff., Fabaceae undiff., Geraniaceae undiff., <i>Carya, Euonymus</i> , Ranunculaceae undiff., Rosaceae undiff., Rubiaceae undiff., Saxifragaceae undiff., Solanaceae undiff., Urticaceae undiff.
Aquatics	<i>Typha/Sparganium, Isoetes</i> type, <i>Cyperaceae</i> undiff., <i>Thalictrum, Nymphaea</i>

type = plausible taxonomic attribution based on morphology

undiff. = undifferentiated

220

221 3.3. Statistical methods

222 Zonation in the pollen diagram was achieved by using the Constrained Incremental Sum-of-
 223 Squares (CONISS) cluster analysis method, based on the TLP. Zone 976-VIII-10 was added
 224 manually, based on visual observation of the CONISS results and changes in the pollen
 225 assemblage which needed highlighting. To help visualise the results from the pollen analysis,
 226 Principal Component Analysis (PCA) was implemented using PAST (Paleontological Statistic)
 227 (Hammer *et al.*, 2001). PCA plots show the distribution of samples and the loadings of the
 228 ecological groups, achieved by summing the percentages of the taxa in each group (table 2).
 229

230 4. Results

231 4.1 Pollen analysis

232 Pollen analysis on the marine sequence ODP976 produced a high-resolution continuous
 233 record spanning the timeframe between 434 and 356 ka BP (MIS 12 to MIS 10), with an
 234 average temporal resolution of 480 years. A higher average temporal resolution of 128 years
 235 between samples was achieved in the portion representative of the transition MIS 12/11,
 236 while the depths representative of the end of MIS 11 and initiation of MIS 10 have a lower
 237 resolution of 400 years.

238 The average TLP count for each sample was 160.8, and only in 6 samples the target of
 239 150 pollen grains was not reached (75–142 grains). The total sum of counted pollen grains for
 240 all the samples was 22,680 (not including *Pinus*). The average number of taxa included in the
 241 TLP for each sample was 21. In total, 89 pollen taxa were identified. *Pinus* was found to be
 242 overrepresented as in many other studies in the region, with a total sum of 42,061 pollen
 243 grains for all the samples. Absolute concentrations of land pollen (excluding *Pinus*) have a
 244 range of 2,964–76,473 grains/g, with the highest values occurring in two intervals at 116.55–
 245 117.08 m and 107.3–110.1 m. Pollen preservation was good throughout the core considering
 246 its marine origin, with 0.5–9% of pollen considered indeterminable.

247 Pollen zonation through CONISS revealed eight palynologically distinctive zones,
 248 summarised in Table 3. The percentage pollen diagram in Figure 4 shows taxa with
 249 abundances over 5%.

250 Pollen assemblages show a clear shift from a high abundance of *Pinus*, pioneer and
 251 steppic taxa in zone 976-I-12 to an assemblage comprised of temperate and Mediterranean
 252 taxa in zone 976-II-11. In zone 976-III-11, *Quercus deciduous* replaces *Pinus* as the dominant
 253 taxon and temperate and Mediterranean taxa reach their maximum levels. In zone 976-IV-11,
 254 temperate and Mediterranean taxa still represent the dominant proportion of the pollen
 255 assemblage, but towards the top of the zone *Q. deciduous* and *Q. ilex* slowly decline while
 256 *Artemisia*, *Cedrus* and *Pinus* increase. In zone 976-V-11 there is a shift from temperate and
 257 Mediterranean taxa to a higher abundance of *Pinus*, *Cedrus* and steppic taxa. There is a
 258 renewed increase in temperate taxa in zone 976-VI-11, but Mediterranean taxa remain low
 259 and high abundances of *Pinus* and *Cedrus* persist. From zone 976-VII-11 to 976-VIII-10, there
 260 is a continuous decrease in temperate and Mediterranean taxa and an increase in *Pinus*,
 261 montane and steppic taxa.
 262

Table 3 – Description of pollen assemblage zones.

Zone	Depth (m)	Age (ka BP)	Pollen description
976-VIII-10	98.85– 100.85	356.456– 365.343	<i>Pinus</i> reaches abundances up to 77%. <i>Cedrus</i> is very abundant 22–36%. Decrease in temperate taxa (<i>Q. deciduous</i> 4–20%) and Mediterranean taxa appear only sporadically (<i>Q. ilex</i> <2%). Herbaceous and pioneer taxa are present at <10%. <i>Isoetes</i> spores decrease and disappear at the end of the zone.
976-VII-11	100.85– 105.5	365.343– 386.005	Increase in <i>Pinus</i> (>60%), montane (<i>Cedrus</i> >20%) and steppic taxa (<i>Artemisia</i> >10%). Decrease in temperate and Mediterranean taxa. <i>Q. deciduous</i> declines (<20%). <i>Q. ilex</i> decreases to <4% and other Mediterranean taxa (<i>Olea</i> , <i>Cistus</i>) decline to <2%. Herbaceous taxa are consistently present, and pioneer taxa (<i>Cupressaceae</i> and <i>Centaurea</i>) are present at low rates. <i>Isoetes</i> spores decrease to less than 10%.
976-VI-11	105.5– 108.95	386.005– 399.435	Slight increase in temperate (<i>Q. deciduous</i>) and herbaceous taxa (<i>Cichorioideae</i>). Mediterranean taxa remain at very low rates (<i>Q. ilex</i> , <i>Cistus</i> and <i>Phillyrea</i> occur at abundances <5%). <i>Olea</i> appears sporadically at abundances <3%. <i>Pinus</i> (20–40%), <i>Cedrus</i> (15–20%)

			and steppic taxa (<i>Artemisia</i> , Chenopodiaceae and <i>Ephedra</i>) undergo a slight decline but remain dominant. Cupressaceae occur at rates around 3%. <i>Isoetes</i> spores increase, reaching levels around 15%.
976-V-11	108.95– 110.03	399.435– 403.140	Temperate and Mediterranean taxa decline to half their previous abundance (<i>Q. deciduous</i> 10%, <i>Q. ilex</i> 2%). All other Mediterranean and temperate taxa decrease to near zero values except for <i>Cistus</i> which persists at an abundance of 3–5%. <i>Pinus</i> rises to over 60%. Increase in abundance of montane (<i>Cedrus</i> 30–40%) and steppic taxa (<i>Artemisia</i> 20%). Chenopodiaceae and <i>Ephedra</i> also increase. Poaceae remains constantly abundant (10–15%). Herbaceous taxa decrease (Cichorioideae and c.f. <i>Erica arborea</i>). <i>Isoetes</i> spores decline (<2%).
976-IV-11	110.03– 112.11	403.140– 410.277	<i>Q. deciduous</i> is the most dominant taxon, although it undergoes a steady decline with two significant drops at 111.74m (27%) and 110.28m (23%). <i>Q. ilex</i> decreases in this zone (5–11%). <i>Olea</i> decreases to an average of 4%. <i>Cistus</i> becomes more consistently present (2–6%). <i>Pinus</i> abundances remain low (5–15%) but increase slightly towards the top of the zone (23%). Herbaceous taxa become increasingly prevalent (Asteroideae up to 10%, Cichorioideae average 24%). Steppic taxa (Poaceae) are abundant at the beginning of the zone (up to 14%) before decreasing to <10% at the top. <i>Isoetes</i> spores reach their maximum abundance (17–26%).
976-III-11	112.11– 115.89	410.277– 423.227	<i>Q. deciduous</i> is the most abundant taxon (up to 51%), peaking above 45% at 113.02 m, 112.74 m, 112.26 m and 112.16m. <i>Q. ilex</i> also reaches its maximum abundance (peaks >15% at 113.94 m, 113.34 m and 113.02 m). <i>Olea</i> abundance is low but continuous (5–8%). Other Mediterranean taxa including <i>Phillyrea</i> and <i>Cistus</i> occur intermittently. <i>Pinus</i> declines to 15–20%. Abundances of riparian taxa are low, with <i>Salix</i> representing the most continuous taxon. Pioneer and steppic taxa are low (<10%). <i>Cedrus</i> appears intermittently below 2%. Cichorioideae remain abundant (up to 19%). Pioneer taxa abundances are only present sporadically at low abundances, while steppic taxa show continuous abundances. <i>Isoetes</i> spores increase (15–20%).
976-II-11	115.89– 116.93	423.227– 426.648	Temperate and Mediterranean taxa increase rapidly, while the abundances of montane, pioneer and steppic taxa decrease drastically. <i>Pinus</i> declines from 52% to 24%, <i>Cedrus</i> declines to less than 5%. <i>Quercus deciduous</i> increases to 30%. Riparian taxa (<i>Salix</i> and <i>Betula</i>) are present at low abundances. <i>Quercus ilex</i> (4–8%) and <i>Olea</i> (6–17%) make up the majority of Mediterranean taxa. Herbaceous taxa are abundant (Cichorioideae 15% and c.f. <i>Erica arborea</i> 8%). Cupressaceae decrease to 1–2%, while steppic taxa decline to <10%. <i>Isoetes</i> spores increase slightly.
976-I-12	116.93– 118.8	426.688– 433.868	<i>Pinus</i> is abundant (46–86%) with a peak at 118.14 m. <i>Cedrus</i> is abundant (up to 17%). <i>Picea</i> and <i>Abies</i> are present. <i>Quercus deciduous</i> is low (< 10%). Mediterranean taxa are mostly absent, except for individual grains of <i>Phillyrea</i> and <i>Cistus</i> . Herbaceous taxa are prevalent throughout, predominantly Cichorioideae (up to 28%). Pioneer (Cupressaceae 10%) and steppic taxa (<i>Artemisia</i> up to 29%, Poaceae 10–30%, <i>Ephedra distachya</i> and <i>Ephedra fragilis</i> up to 10%) are abundant.

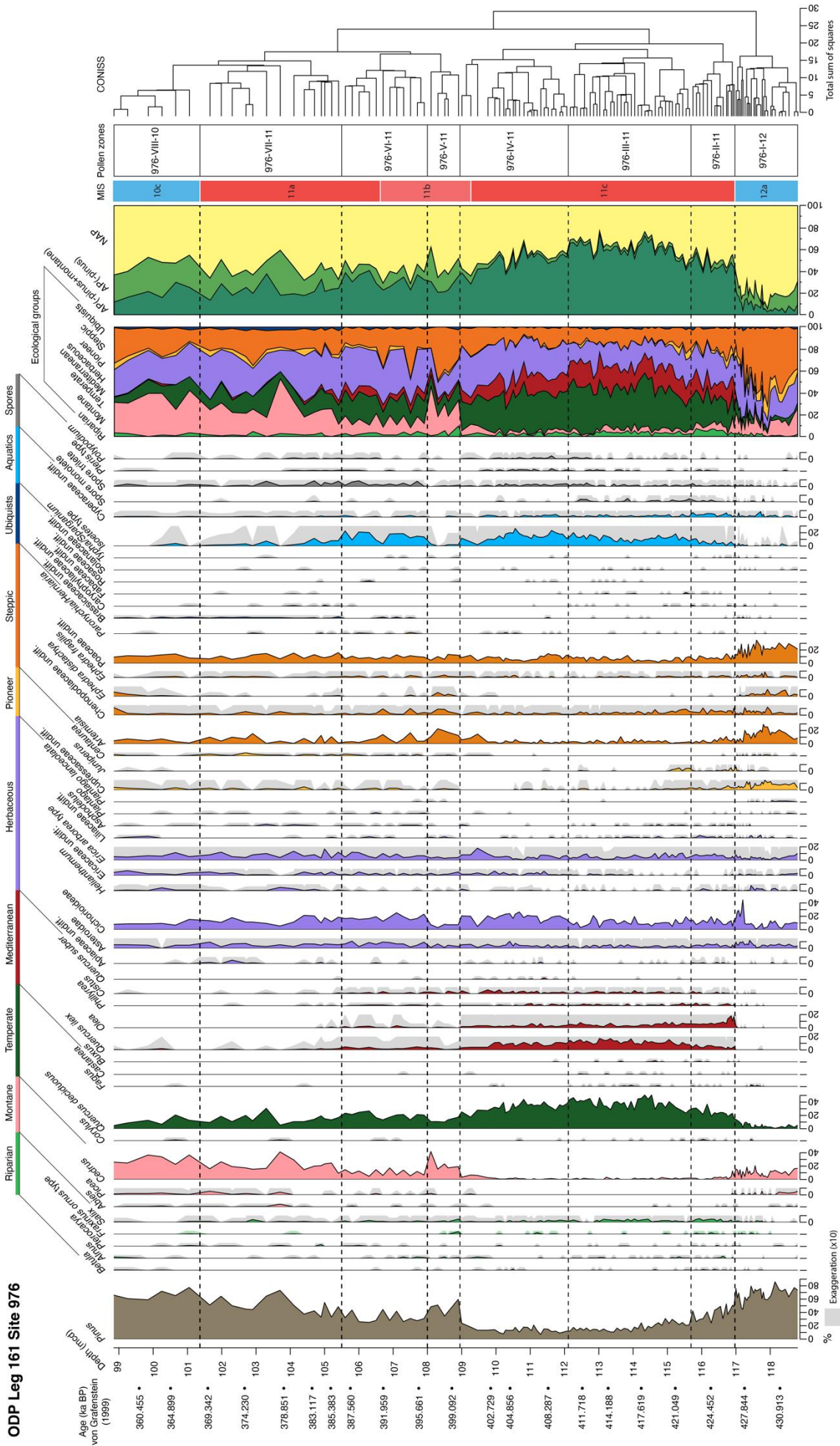


Figure 4 — Pollen percentage diagram for ODP Site 976, showing taxa reaching >5% abundance plotted against depth. On the left, ages (in ka BP) from von Grafenstein *et al.* (1999) are plotted according to meters composite depth (mcd). Synthetic diagrams showing the ecological groups and AP/NAP pollen curves are shown on the right. Pollen zones with CONISS clustering, and MIS stage equivalents, are shown on the far right. Data for taxa <5% is available in the supplementary data. Grey curves in the background indicate the x10 exaggeration.

264 **4.2 PCA analysis**

265 PCA of the ecological groups, excluding *Pinus*, aquatics and spores (Fig. 5A), found that PC1
 266 represents 64% of the total variance while PC2 represents 20%. Samples appear to be broadly
 267 clustered according to the zonation produced through CONISS. Zones 976-I-12, 976-VI-11,
 268 976-VII-11 and 976-VIII-10 are primarily found on the left of the biplot with negative values in
 269 PC1, and their variance is also represented in PC2 with scores ranging from -30 to 30. These
 270 samples appear to be influenced mainly by montane (*Cedrus*, *Picea*), steppic (*Juniperus*,
 271 Poaceae, Cupressaceae) and pioneer groups (*Artemisia*). Zone 976-II-11 is clustered close to
 272 the centre of the PCA plot, and seems to be influenced primarily by the riparian and pioneer
 273 taxa (mainly *Ephedra distachya*, Chenopodiaceae and Cupressaceae). Zones 976-III-11, 976-
 274 IV-11 and 976-V-11 are mostly clustered to the left of the diagram with primarily negative
 275 scores in PC1 and are limited within a range of -7.5–7.5 in PC2. These zones appear to be
 276 primarily influenced by temperate and Mediterranean groups (*Q. deciduous*, *Q. ilex*, *Cistus*
 277 and *Olea*).

278 A more focused PCA was also run on the samples from zones 976-II-11 to 976-VII-11
 279 assumed to represent the MIS 11 interglacial (Fig. 5B), achieved by removing zones
 280 significantly influenced by montane and steppic taxa (976-I-12 and 976-VIII-10). In this plot,
 281 PC1 represents 59% of the total variance while PC2 represents 18%. The clustering of the
 282 samples reveals significant differences between these zones. Zone 976-II-11 remains
 283 distributed around the middle of the biplot, with predominantly negative scores in PC2 and
 284 influenced by pioneer, riparian and steppic taxa. Zone 976-V-11 also is distributed closer to
 285 the centre of the plot, but appears to be more influenced by herbaceous taxa and has more
 286 positive scores in PC2. Zones 976-III-11 and 976-IV-11 are clustered on the right, although
 287 zone 976-III-11 is predominantly influenced by temperate and Mediterranean taxa while zone
 288 976-IV-11 is more influenced by ubiquist taxa. Meanwhile, zones 976-VI-11 and VII are
 289 distributed to the left and are similarly influenced by herbaceous and montane groups,
 290 although zone 976-VII-11 has overall more negative scores in PC1.

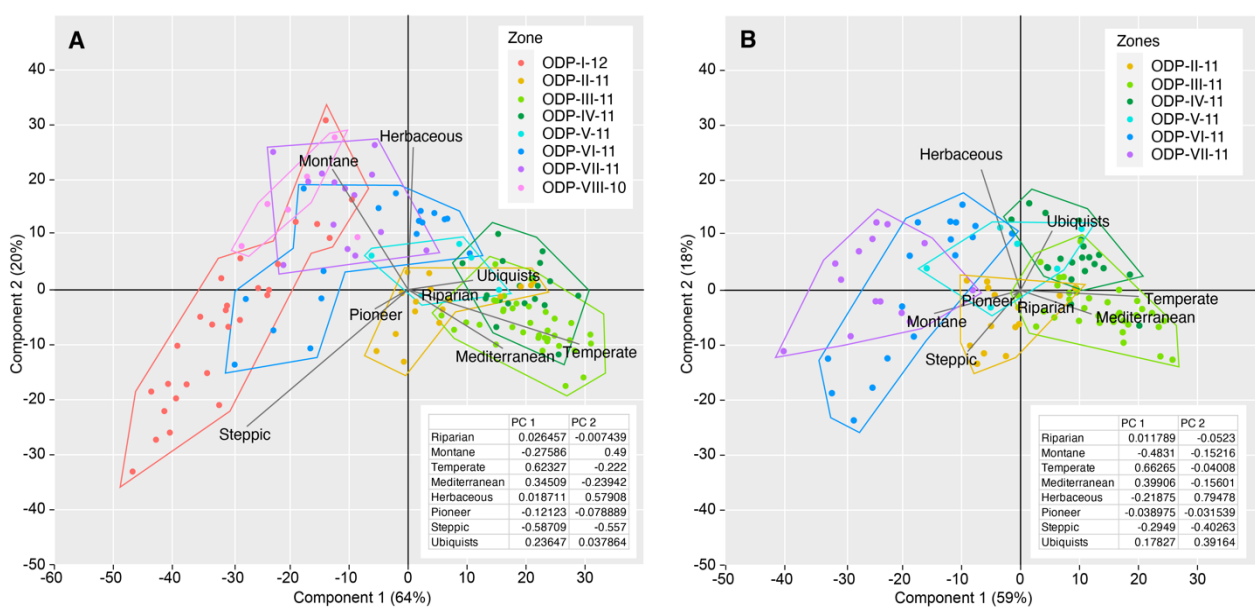


Figure 5 – Principal Component Analyses (PCA) of samples from (A) the entire record and (B) samples only from zones 976-II-11 to 976-VII-11, showing their distribution in relation to ecological groups. *Pinus*, aquatics and spores have been omitted from the analysis. Loadings of the ecological groups for PC1 and PC2 are presented in the bottom right of each plot.

291 **5. Discussion**

292 **5.1 Palaeoenvironmental interpretations**

293 Pollen results in the lowermost zone of this record (976-I-12), representing the period
294 between 434 and 427 ka BP, show that the assemblage is dominated by *Pinus*, high
295 abundances of steppic and pioneer taxa such as Poaceae, Cupressaceae, *Artemisia*, *E.*
296 *distachya* and *E. fragilis*, suggesting that a cold climate prevailed in the region consistent with
297 the MIS 12 glacial period. These conditions would have limited the establishment of
298 temperate trees leaving a semi-desertic landscape characterised mainly by shrubs at the
299 lower altitudes of the Mediterranean (Hes *et al.*, 2022). At mid- and higher altitudes, *Pinus*
300 and other montane taxa (mainly conifers, i.e. *Cedrus* and *Picea*) would have prevailed.

301 An abrupt climatic shift is observed between zones 976-I-12 and 976-II-11, in which *Pinus*,
302 montane, pioneer and steppic decrease drastically and are replaced by arboreal associations
303 composed of riparian, temperate and Mediterranean taxa (Fig. 6A). This is a clear indication
304 of the transition between MIS 12 and 11, observed specifically around 426 ka BP. The onset
305 of assemblages comprised of *Salix*, *Quercus deciduous*, *Q. ilex* and *Olea* suggests a rapid
306 climatic amelioration towards a warmer and more humid setting. Particularly, the marked rise
307 in *Olea* at this time, a genus typical of the thermo-Mediterranean belt and commonly
308 associated with warm interglacials of the Pleistocene and Holocene (Punt and Blackmore,
309 1991; Quézel and Medail, 2003), is indicative of a significant rise in temperatures.
310 Furthermore, the gradual increase in *Isoetes*, a taxon which is related to marshlands and
311 freshwater, is suggestive of higher precipitation associated with the transition from glacial to
312 interglacial (Sánchez Goñi *et al.*, 1999). The amplitude of the transition observed in this record
313 is in line with the overall consensus that Termination V represents an extreme climatic shift
314 (Droxler *et al.*, 2003).

315 The expansion of the temperate and Mediterranean forest in zones 976-III-11 and IV, and
316 the consistently low percentages of *Pinus*, pioneer and steppic taxa, correspond to the period
317 between 423 and 403 ka BP which can be correlated with the long and warm climatic
318 optimum MIS 11c. The results are consistent with intense warmth and elevated humidity also
319 recognised in other terrestrial and marine Mediterranean records (Oliveira *et al.*, 2016; Kousis
320 *et al.*, 2018; Azibeiro *et al.*, 2021). Specifically, the period represented by zone 976-III-11 (423–
321 410 ka BP) exhibits the highest abundance of temperate and Mediterranean taxa in the entire
322 record, an assemblage made up mostly of *Q. deciduous*, *Q. ilex*, *Olea*, *Phillyrea* and *Cistus*
323 occurring along a continuous high abundance of *Isoetes*. This period represents the warmest
324 phase recorded, consistent with the MIS 11c climatic optimum. This is followed by a gradual
325 decline in temperate and Mediterranean taxa throughout zone 976-IV-11, representing the
326 latter part of MIS 11c (410–403 ka BP). Although in decline, the temperate forest still
327 represents the dominant proportion of the assemblage and the rates of *Q. ilex* are still
328 relatively high compared to the previous zone. Combined with the high abundances of *Isoetes*
329 and the low rates of pioneer and steppic taxa, this indicates that the climate was
330 predominantly warm and wet.

331 The slowly decreasing trends of *Q. deciduous* and Mediterranean taxa and the increase
332 in *Pinus* and *Cedrus* towards the upper part of zone 976-IV-11, around ca. 400 ka BP, may
333 indicate the onset of a cooler phase recognised in other studies as MIS 11b (Desprat *et al.*,
334 2006; Oliveira *et al.*, 2016; Kousis *et al.*, 2018; Ardenghi *et al.*, 2019). In zone 976-V-11, the
335 shift observed from temperate and Mediterranean taxa to an assemblage comprising *Pinus*,
336 *Cedrus*, and steppic taxa (*Artemisia*, Chenopodiaceae, *E. distachya* and *E. fragilis*) is indicative
337 of a decline in temperature and an increase in aridity. The persistence of *Q. deciduous* and

338 some Mediterranean taxa (e.g. *Q. ilex*, *Olea*, *Cistus*, although at abundances <3%) suggest that
339 the climate was still viable for the presence of humid forests, but not warm or moist enough
340 to support the high forest cover seen during the optimum, leading to a significant forest
341 contraction. The expansion of *Cedrus* at mid-altitude, the increase of *Artemisia* and the
342 decline of *Isoetes* are particularly indicative of a drier climate which would have been too
343 harsh for temperate and Mediterranean trees, leading to colonisation by conifers and shrubs
344 typical of a cool period.

345 This cooler phase is followed by a renewed increase in temperate taxa and a minimal rise
346 in Mediterranean taxa, observed in zone 976-VII-11, indicating a new period of forest
347 expansion. Together with the increase in *Isoetes*, this may be interpreted as a return of warm
348 and humid conditions suitable for the expansion of a temperate forest, albeit reduced
349 compared to the climatic optimum as suggested by the persistently higher abundances of
350 *Pinus*, *Cedrus* and *Artemisia*. This phase is consistent with the conditions of MIS 11a, which is
351 often recognised as a period of transition from temperate deciduous to cold mixed forests
352 (Kousis *et al.*, 2018) indicative of high climatic variability (Candy *et al.*, 2014).

353 The uppermost zones, 976-VII-11 and VIII-10 (386–356 ka BP), encompass the transition
354 from MIS 11 to the glacial MIS 10. The end of MIS 11a is characterised by large fluctuations in
355 the temperate and montane forests, with a particular phase of contraction in *Q. deciduous*
356 and an expansion of *Pinus* and *Cedrus* around 380 ka BP. This particular event occurs without
357 an increase of steppic and pioneer taxa suggesting that a semi-arid shrubland did not develop
358 and therefore this was a predominantly cold event not subject to a change in humidity. Such
359 an increase in conifers, especially *Cedrus*, without a particular increase in semi-desert taxa,
360 may also signify a probably enhanced wind input from the south of the Alboran Sea associated
361 with the settling of montane forests in the high-altitudes of the Betic and Rif Arc mountains
362 (Magri and Parra, 2002; Bout-Roumazeille *et al.*, 2007; Combourieu-Nebout *et al.*, 2009). This
363 period is followed in zone 976-VIII-10 by a steady decline in *Q. deciduous* and a very sporadic
364 appearance of Mediterranean taxa, consistent with the long-term cooling trend towards MIS
365 10 (McManus *et al.*, 2003; Oliveira *et al.*, 2016). *Pinus* and *Cedrus* become the dominant taxa,
366 accompanied by a rise in Cupressaceae, Chenopodiaceae and *E. distachya*, which is
367 interpreted as the return of glacial conditions at the onset of MIS 10 around 367 ka BP,
368 characterised by a predominantly montane forest and herbaceous/steppic assemblages.
369

370 5.2 MIS 12/11 transition

371 The shift in vegetation recorded in ODP976 between 430 and 425 ka BP, characterised by the
372 sharp transition from *Pinus*, montane and steppic taxa to temperate and Mediterranean
373 assemblages, represents the period of climatic change from the cold and arid conditions of
374 MIS 12 to the warm and humid conditions of MIS 11. This transition has been documented in
375 several palaeoenvironmental and palaeoclimatic records from the Mediterranean (Tzedakis
376 *et al.*, 2001; Girone *et al.*, 2013; Kousis *et al.*, 2018; Ardenghi *et al.*, 2019; Azibeiro *et al.*, 2021),
377 the North Atlantic off the Iberian coast (Desprat *et al.*, 2005; Oliveira *et al.*, 2016) and
378 continental Europe (Reille and de Beaulieu, 1995). The timing of the transition is largely
379 synchronous across the records in the Mediterranean and North Atlantic and has been
380 identified between 428 and 424 ka BP (Figs. 6 and 7).

381

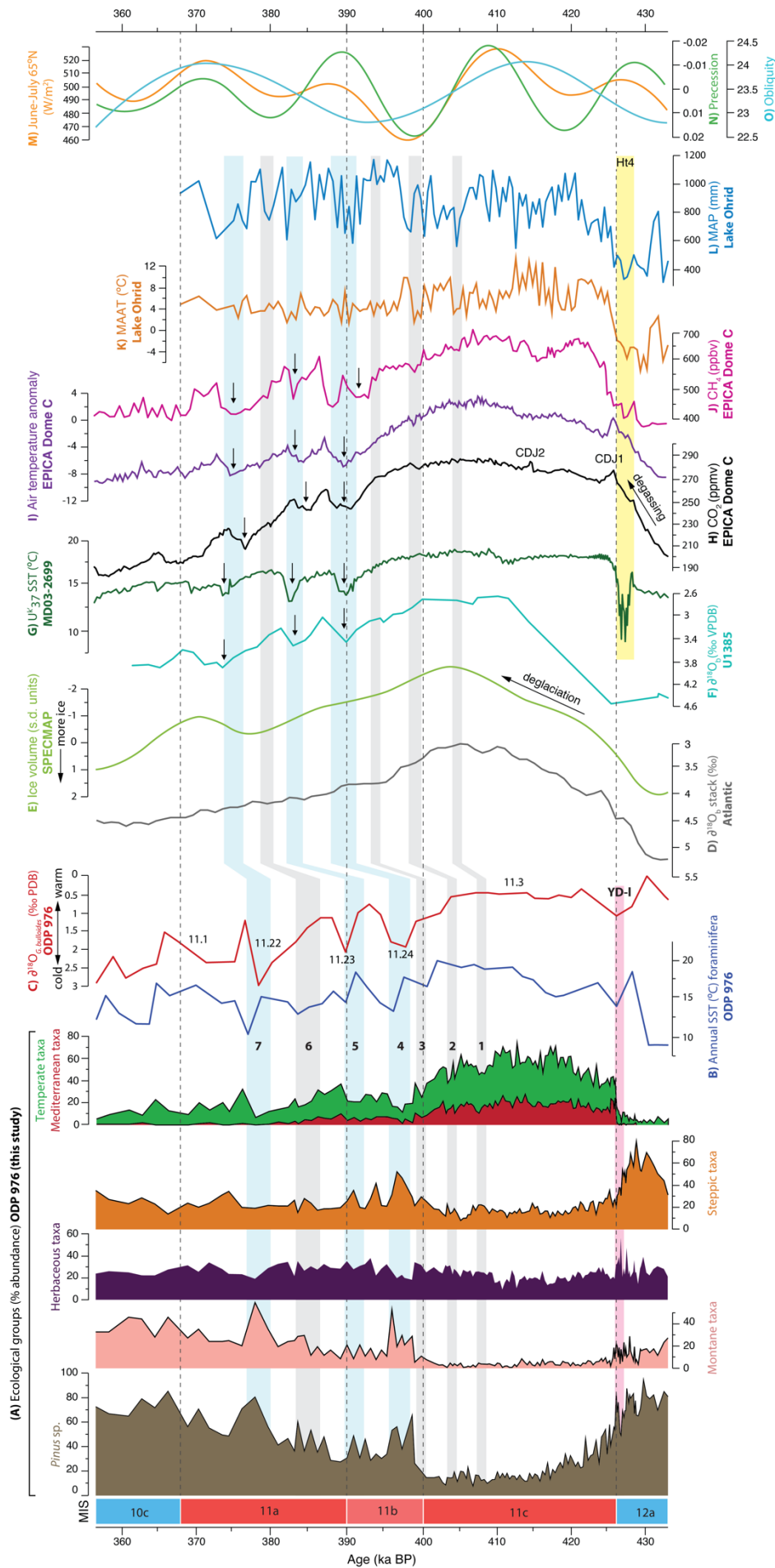


Figure 6— Comparison between (A) selected ecological groups from the ODP Site 976 record in this study, and proxies of climatic variability: (B) Annual SSTs from function transfer of foraminiferal assemblages and (C) $\delta^{18}\text{O}_{\text{G. bulioides}}$ from ODP Site 976 (Brice, 2007), with numbered light and heavy isotopic events after Bassinot et al. (1994); (D) Benthic $\delta^{18}\text{O}$ stack from the Atlantic (Lisiecki and Raymo, 2009); (E) Ice volume from SPECMAP stacked $\delta^{18}\text{O}$ (Imbrie et al., 1984); (F) Benthic $\delta^{18}\text{O}$ from U1385 (Oliveira et al., 2016); (G) Alkenone SSTs from MD03-2699 (Rodrigues et al., 2011); (H) CO_2 atmospheric concentrations from Antarctic EPICA Dome C ice core (Nehrbass-Ahles et al., 2020); (I) Antarctic air temperature anomaly from Antarctic EPICA Dome C ice core (Jouzel et al., 2007); (J) Methane (CH_4) atmospheric concentrations from Antarctic ice cores EDC (Loulergue et al., 2008); (K) Mean annual temperature and (L) Mean annual precipitation reconstructions from Lake Ohrid (Kousis et al., 2018); (M) Summer insolation (Laskar et al., 2004); (N) Precession index and (O) Obliquity curve (Berger and Loutre, 1991). All curves are plotted within their original chronological framework. Numbered bands indicate millennial-scale forest contractions of high (blue bands 4, 5 and 7) and moderate intensity (grey bands 1, 2, 3 and 6). The light pink band indicates the Younger Dryas-like event, while the yellow band highlights the Ht4 event observed in other records.

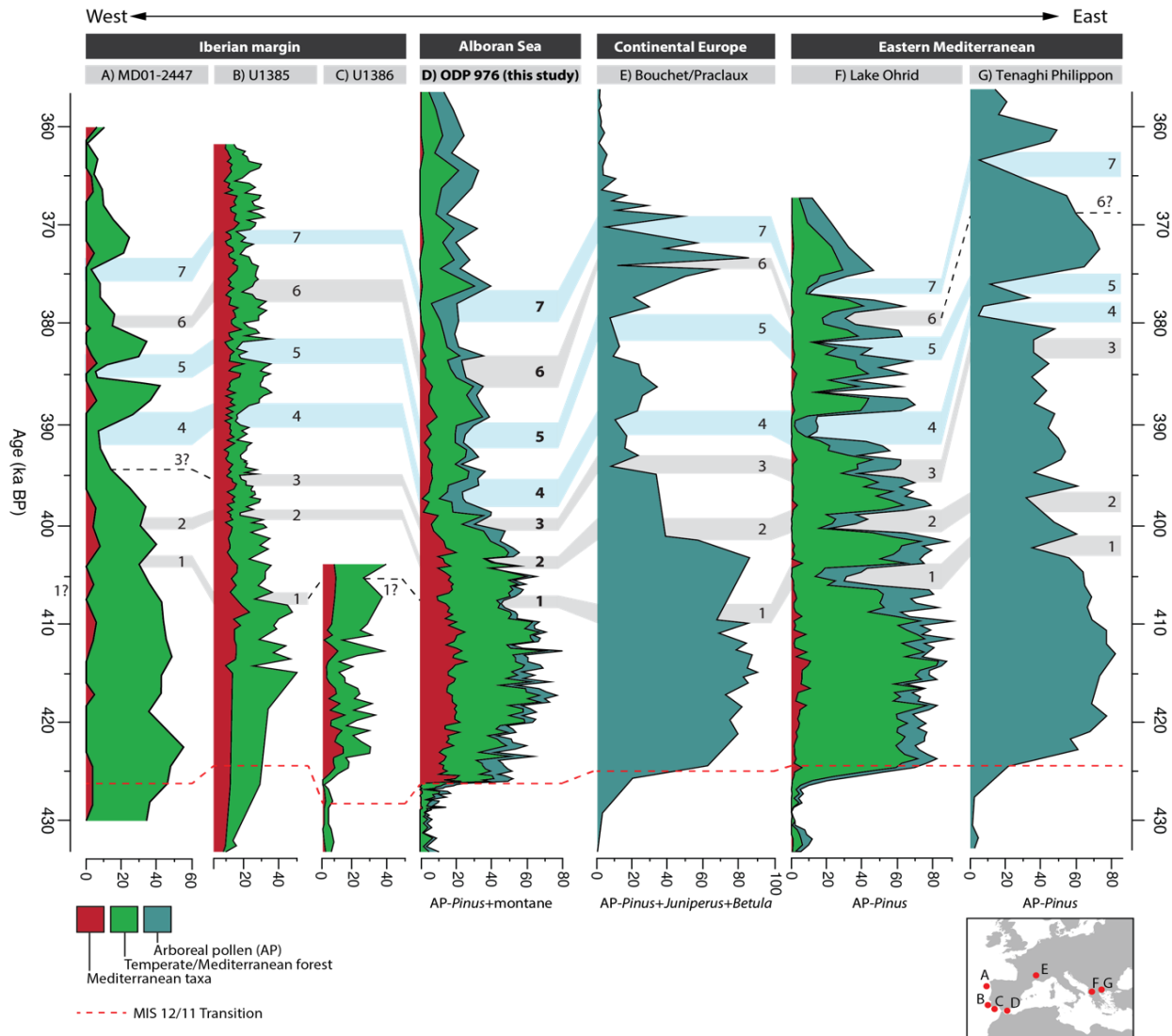


Figure 7 – Comparison of the AP curves and the Mediterranean and temperate ecological groups of high-resolution pollen records from the Mediterranean which encompass MIS 12 and 11: (A) Marine site MD01-2447 (Desprat *et al.*, 2005); (B) Marine site IDOP U1385 (Oliveira *et al.*, 2016); (C) Marine site IODP U1386 (Hes *et al.*, 2022); (D) Marine site ODP 976 (this study); (E) Bouchet/Praclaux (drawn after Reille and de Beaulieu, 1995); (F) Lake Ohrid (Kousis *et al.*, 2018); (G) Tenaghi Philippon (Ardenghi *et al.*, 2019). Coloured bands indicate the millennial-scale forest contraction events identified in Figure 6, and the tentative correlations made with the other records. Dotted line indicates a correlation where no analogue was identified. All records are plotted within their original chronological framework.

383 The changes observed in our pollen record coincide with independent Sea Surface
 384 Temperature (SST) reconstructions and planktonic $\delta^{18}\text{O}_{\text{Globigerina bulloides}}$ records derived from
 385 ODP976 (Fig. 6B and C) by Brice (2007), which show an overall increase from around 9 to 17°C
 386 between 432 and 427 ka BP, and a drop in $\delta^{18}\text{O}$ values from 1 to nearly 0‰ around 430 ka BP
 387 (Brice, 2007). This decrease in $\delta^{18}\text{O}_{\text{G. bulloides}}$ and the associated rise in SSTs were also detected
 388 in several other marine records from the North Atlantic and Iberian Margin (e.g. Jouzel *et al.*,
 389 2007; Voelker *et al.*, 2010; Vázquez Riveiros *et al.*, 2013; Oliveira *et al.*, 2016) as well as in the
 390 Mediterranean at sites ODP 975 (Girone *et al.*, 2013) and ODP 977 (Azibeiro *et al.*, 2021),
 391 showing a coeval response of these regions to global climatic change. Specifically, this trend
 392 is indicative of the inflow of meltwater from the North Atlantic into the Strait of Gibraltar as
 393 a result of the decrease in ice volume caused by increasing insolation (Hes *et al.*, 2022; Candy

394 *et al.*, 2014), as corroborated by the SPECMAP isotopic stack record (Fig. 6E) (Bassinot *et al.*,
395 1994; Imbrie *et al.*, 1984).

396 This trend of climatic amelioration is interrupted by an abrupt return to colder and drier
397 conditions around 428–426 ka BP as evidenced by the sudden decrease SSTs and an episode
398 of rapid increase in $\delta^{18}\text{O}_{G. bulloides}$ (Brice, 2007), which corresponds with a coeval and short-
399 lived increase in *Pinus*, montane taxa and herbaceous taxa (Cichorioideae) at the expense of
400 temperate taxa at 427 ka BP, at the interface between MIS 12 and 11 (Fig. 6). Brice (2007)
401 defines this interval as a Younger Dryas-like event (YD-I), given its resemblance to the event
402 following the last deglaciation between 12.9 and 11.5 ka BP. Other studies have identified a
403 prominent cold phase during the transition, and have sometimes referred to as Heinrich-type
404 event Ht4 (Hodell *et al.*, 2008; Rodrigues *et al.*, 2011; Girone *et al.*, 2013; Marino *et al.*, 2018).
405 Vázquez Riveiros *et al.* (2013) observed a pulse of enhanced Ice Rafted Debris (IRD) in their
406 record from ODP980 between 430 and 425 ka BP, synchronous with a sharp reduction in
407 North Atlantic SSTs, suggesting a substantial ice-rafting event accompanied by a large
408 production of brine waters during this time. This phase was also recorded by Rodrigues *et al.*
409 (2011) in their alkenone-derived SST record from core MD03-2699 (Fig. 6G) and by Regattieri
410 *et al.* (2016) in their $\delta^{18}\text{O}$ record from the Sulmona basin in central Italy, showing similar
411 responses in marine and terrestrial records. These events are common in many North Atlantic
412 records (e.g. McManus *et al.*, 1999; Voelker *et al.*, 2010) and are related to major ice-sheet
413 instability during periods of climate reorganisation (Regattieri *et al.*, 2016). This phase is also
414 corroborated by the pollen-based reconstructions by Kousis *et al.* (2018) for Lake Ohrid which
415 show a decrease in mean annual atmospheric temperatures (MAAT; Fig. 6K) and mean annual
416 precipitation (MAP; Fig. 6L), and a phase of reduced forest cover in their pollen record at this
417 site between 430 and 427 ka BP (Fig. 7). However, while the Ht4 stadial recognised in other
418 records is generally understood as a cold and dry event, the peak of Cichorioideae in our
419 record leads to the interpretation of a cold but rather humid event in this part of the
420 Mediterranean. As suggested by several authors (e.g. Vázquez Riveiros *et al.*, 2013; Tzedakis
421 *et al.*, 2022), the influx of freshwater caused by the deglaciation led to a weakening of the
422 Atlantic Meridional Overturning Circulation (AMOC), which may have been caused by the
423 activation of a bipolar see-saw pattern in precipitation between the western and eastern
424 Mediterranean.

425 The YD-I/Ht4 event decreased the cooling effect of cold water upwelling as a result of the
426 weakened AMOC, in turn leading to the further warming of Antarctica (Tzedakis *et al.*, 2022).
427 This is visible in panels H, I and J in Figure 6, which show the steady increase in the CO_2 , air
428 temperature and methane (CH_4) records from the Antarctic EPICA Dome C ice cores (Jouzel
429 *et al.*, 2007; Loulergue *et al.*, 2008; Nehrbass-Ahles *et al.*, 2020). This exceptional warming
430 and increase in greenhouse gas concentrations may explain the high biosphere productivity
431 and the major increase in global forest biomass during Termination V (Brandon *et al.*, 2020).
432 Among the pollen records from the Mediterranean and continental Europe, the onset of MIS
433 11c is represented by a pronounced phase of forest expansion (Fig. 7). Though the specific
434 timing of this increase in forest cover is slightly different, possibly due to discrepancies
435 between chronologies, this response is likely to have been caused by a large uptake of
436 atmospheric CO_2 during the degassing period (Tzedakis *et al.*, 2022). The peak in CO_2 at 426
437 ka BP—also known as the first ‘Carbon Dioxide Jump’ (CDJ) (Tzedakis *et al.*, 2022)—and the
438 concomitant peak in Antarctic air temperatures, are particularly important as they correlate
439 with the dramatic rise in *Olea* and *Q. ilex* at this time in the ODP976 record. This interpretation
440 is in agreement with pollen-based climatic reconstructions from Lake Ohrid, which suggest a

441 transition towards wetter and warmer conditions at the onset of MIS 11c, evidenced by a rise
442 in MAAT by 7°C and in MAP by 150 mm at Lake Ohrid (Kousis *et al.*, 2018). The development
443 of more Mediterranean conditions around the lower latitudes of the Alboran Sea during this
444 time would have been necessary for the expansion of evergreen forests (Okuda *et al.*, 2001).

445 Regionally, our results are in agreement with palynological records from Lake Ohrid
446 (Kousis *et al.*, 2018), Tenaghi Philippon (Wijmstra and Smit, 1976; Tzedakis *et al.*, 2006;
447 Ardenghi *et al.*, 2019) and Bouchet/Praclaux (Reille and de Beaulieu, 1995), which show a
448 synchronous expansion of forest biomass throughout Termination V. This overall trend is
449 corroborated by palaeoclimatic data from the North Atlantic and Mediterranean which record
450 increasing SSTs, CO₂, CH₄ and a significant drop in δ¹⁸O. These patterns are significant because
451 they demonstrate analogous changes in vegetation in terrestrial and marine records during
452 this period. Nevertheless, a close comparison with the high-resolution pollen record of Lake
453 Ohrid reveals that the amplitude of change in Mediterranean vegetation at ODP976 during
454 the MIS 12/11 transition is significantly greater. This could suggest that the ODP976 record
455 reflects a warmer and drier climate at the onset of MIS 11c in the southwestern
456 Mediterranean compared to the Balkan Peninsula where Lake Ohrid is located. Due to the
457 higher altitude of Lake Ohrid (1514 m asl) and its geomorphological context, however, this
458 site may be recording a more local signal from a subdued Mediterranean forest, while the
459 ODP976 marine record is likely to represent a wider regional signal of the vegetation changes
460 occurring around the Alboran sea.

461

462 5. 3 MIS 11 vegetation and climatic variability

463 5.3.1 Long-term vegetation and climate change

464 Evaluation of the pollen data indicates that MIS 11c was the warmest substage, characterised
465 by the maximum forest extent consistent with a climatic optimum between 426–400 ka BP,
466 observed ubiquitously across palaeoenvironmental and palaeoclimatic records. This substage
467 is often characterised by the largest expansion of mixed oak forest and Mediterranean taxa
468 (Fig. 6), concurrent with the results from ODP976. This forest expansion, also referred to as
469 the ‘Sines’ forest phase in marine records from the Iberian margin (Oliveira *et al.*, 2016; Hes
470 *et al.*, 2022), reflects the highest degree of warming and seasonal rainfall in the south-western
471 Mediterranean, and is associated with the light isotopic event MIS 11.3 (see Fig. 6C) as well
472 as the strongest Northern Hemisphere summer insolation of the interglacial (Fig. 6M)
473 (Oliveira *et al.*, 2016). The occurrence of warm conditions is particularly supported by the
474 presence of thermophilous taxa such as *Q. ilex*, *Phillyrea* and *Olea*, which require warm and
475 dry summers and mild winters (San-Miguel-Ayanz *et al.*, 2016). Similar findings were reported
476 by Kousis *et al.* (2018) at Lake Ohrid for this period, who showed that annual temperatures
477 for their site reached up to 9.5°C between 415 and 412 ka BP, with mean temperatures for
478 the coldest month (MTCO) around 1.5°C, signifying frost-free winters. Our
479 palaeoenvironmental interpretations correlate well with the highest foraminifera- and
480 alkenone-based SSTs, maximum concentrations of CO₂ and CH₄ from the EPICA ice cores
481 (Jouzel *et al.*, 2007; Nehrbass-Ahles *et al.*, 2020), and diminished δ¹⁸O (e.g. Voelker *et al.*,
482 2010; Oliveira *et al.*, 2016). However, the ODP976 record appears to be subject to a temporal
483 offset from the end of MIS 11c onwards, most possibly caused by differences in dating
484 methods and the development of more precise chronologies in recent years compared to
485 what we have adopted from von Grafenstein *et al.* (1999). Thus, the climatic optimum
486 observed at ODP976 appears shorter than in tuned records where it is usually observed
487 between ~426 and 396 ka BP (Tzedakis *et al.*, 2022). Nevertheless, our record is in agreement

488 with most proxies which show that the duration of MIS 11c averaged around 30 ka (McManus
489 *et al.*, 2003; Tzedakis *et al.*, 2022), and the vegetation signatures are comparable with other
490 pollen records from the region.

491 The exceptional amplitude of response by the temperate and Mediterranean forests to
492 climatic amelioration observed at ODP976 perpetuates the ongoing debate regarding the
493 'Stage-11 problem' or the 'MIS 11 Paradox' (Imbrie *et al.*, 1984; McManus *et al.*, 2003) which
494 refers to the disparity between the strong environmental and climatic response to the weak
495 insolation forcing during this interglacial (Berger and Wefer, 2003). According to Tzedakis *et al.*
496 (2022), the deglaciation during Termination V was significantly prolonged in comparison
497 to other interglacials, as a result of the weak eccentricity-precession forcing and antiphasing
498 between precession (Fig. 6N) and obliquity (Fig. 6O)—i.e. the occurrence of two precession
499 (and insolation) peaks over the course of one obliquity cycle (Tzedakis *et al.*, 2022). This would
500 have protracted the conditions of the interglacial for a period significantly longer than any
501 subsequent interglacial, leading to a rise in summer insolation at both polar regions thereby
502 enhancing the melting of sea ice and allowing more CO₂ outgassing from the North and South
503 Atlantic (Vázquez Riveiros *et al.*, 2013; Tzedakis *et al.*, 2022).

504 The abundances of temperate and Mediterranean taxa reach a maximum between 420
505 and 415 ka BP and remain elevated, in our record, until 410 ka BP, after which they begin to
506 decrease. The long-term forest decline at the end of MIS 11c has also been recorded in other
507 pollen records (Fig. 7) and has been connected to a decrease in summer insolation, showing
508 a regional response of vegetation to solar forcing. These trends also resemble the decline in
509 atmospheric CO₂ and CH₄ records from Antarctica (Jouzel *et al.*, 2007; Loulergue *et al.*, 2008)
510 and the decline in alkenone-based SSTs from the North Atlantic between 415 and 390 ka BP
511 (Fig. 6).

512 The pollen data in the record ODP976 suggests an overall cooling during substage MIS
513 11b (400–390 ka BP) and a return of relatively warmer conditions during MIS 11a (390–367
514 ka BP), though reduced compared to MIS 11c, inferred from the large fluctuations between
515 temperate and montane forests which suggest significant variability in aridity and
516 temperature. These changes are in agreement with the patterns observed in many other
517 palaeoclimatic and palynological records from the North Atlantic and Mediterranean (Candy
518 *et al.*, 2014) and appear to closely follow changes in summer insolation and can be correlated
519 with light isotopic events recognised in $\delta^{18}\text{O}$ records (Fig. 6D, E and F), namely 11.24, 11.23
520 and 11.22 (Desprat *et al.*, 2005; Oliveira *et al.*, 2016). Despite the chronological offset with
521 other records, the pollen data from ODP976 seems to follow insolation and precession cycles
522 more closely than other proxies at other sites. For instance, the increase in *Pinus* and montane
523 taxa during MIS 11b at the expense of temperate and Mediterranean taxa coincides with the
524 insolation and precession minima at 400 ka BP. This supports the idea that, owing to its
525 position in the WAG (see section 2), site ODP976 is sensitive to changes in polar tropical and
526 Atlantic influences caused by climatic variability, and is also a great candidate to observe the
527 influence of the moderate solar forcing of MIS 11 on vegetation.

528

529 5.3.2 Millennial-scale vegetation and climatic variability

530 Following the prolonged and exceptionally stable climatic optimum of MIS 11c, the late part
531 of MIS 11 is characterised by significant millennial-scale oscillations. Previous studies have
532 connected these events with changes in the position of the polar front and the distribution of
533 pressure systems over the North Atlantic during MIS 11 (e.g. Desprat *et al.*, 2007; Oliveira *et al.*
534 *et al.*, 2018, 2016; Sánchez Goñi *et al.*, 2018; Kousis *et al.*, 2018). Two types of such oscillations

535 have been identified: 1) moderate events characterised by distinct declines in forest cover
536 with no counterpart in the SST profiles, and (2) high-intensity events marked by contractions
537 in the temperate and Mediterranean forest synchronous with drops in SSTs and annual
538 atmospheric temperatures (Oliveira *et al.*, 2016; Kousis *et al.*, 2018). Our pollen data
539 documented seven of such pronounced forest contractions (marked by the numbered bands
540 in Figs. 6 and 7), and an attempt has been made to tentatively correlate them with the
541 changes observed in other records from the Mediterranean and North Atlantic (Fig. 7).

542 Four of such moderate-intensity fluctuations in temperate and Mediterranean forest
543 abundance have been identified in our record (grey bands) at ca. 408, 404, 400 and 385 ka BP
544 (events 1, 2, 3 and 6, respectively). The most notable of these oscillations is the first forest
545 contraction, which marks the end of the MIS 11c climatic optimum and has been identified in
546 other pollen records from the region at IODP Site U1385 at 408 ka BP (event U1385-11-fe1;
547 Oliveira *et al.*, 2016), Site MD01-2443 at 406 ka BP (Tzedakis *et al.*, 2009), and at Lake Ohrid
548 between 406.2–404.5 ka BP (event LO-11-1; Kousis *et al.*, 2018). Although it is difficult to
549 locate an equivalent event at the lower-resolution pollen records from Bouchet/Praclaux
550 (Reille and de Beaulieu, 1995) and Tenaghi Philippon (Tzedakis *et al.* 2009) they can be roughly
551 correlated with drops in arboreal pollen around 408 and 402 ka BP, respectively.

552 Oliveira *et al.* (2016) and Kousis *et al.* (2018) have correlated this first forest contraction
553 with the “Older Holstenian Oscillation” (OHO) detected in records from Germany, Denmark,
554 Poland and Britain (West, 1956; Kelly, 1964; Turner, 1970; Kukla, 2003; Koutsodendris *et al.*,
555 2011, 2012; Tye et al 2016). During the OHO, vegetation in western and northern Europe
556 underwent similar changes observed at ODP976, characterised by a strong decline in *Quercus*
557 and *Alnus*. These taxa can tolerate cold conditions but require warm summer and spring
558 (Dahl, 1998), thus indicating in the record a reduction in the temperatures of the warmest
559 months. It is thought that the triggering mechanisms of the OHO were similar to the 8.2 ka
560 event during the Holocene, which was driven by a slowdown of the North Atlantic Deep Water
561 (NADW) formation as a result of increased discharges of meltwater from the Laurentide lakes
562 into the North Atlantic (Barber *et al.*, 1999; Ellison *et al.*, 2006). Climate reconstructions from
563 Lake Ohrid estimate a decrease in MAAT from 8 to 4°C and in MAP from 960 to 550 mm
564 (Kousis *et al.*, 2018). Suggestions regarding the duration of a colder and drier climate during
565 the OHO range between 300 and 780 years (Mangili *et al.*, 2007; Tzedakis *et al.*, 2009).
566 Although its timing is debated (Koutsodendris *et al.*, 2010, 2011, 2012), the detection of a
567 similar contraction in temperate forests in other records at a similar time despite
568 chronological discrepancies points towards a synchronous supraregional response to the OHO
569 and therefore we propose an equivalent interpretation for the changes observed in the
570 ODP976 pollen data.

571 The high-intensity cooling events identified in our record (events 4, 5, 7) are denoted by
572 very pronounced contractions in the temperate and Mediterranean groups and marked
573 increases in *Pinus*, *Cedrus* and steppe taxa. These major cooling events are recognised during
574 MIS 11b and 11a around ca. 397, 390 and 378 ka BP and are synchronous with the three light-
575 isotopic events (11.24, 11.23 and 11.22, respectively) documented by Brice (2007) for ODP976
576 (Fig. 6C). Despite chronological incongruities, equivalent vegetation responses correlated
577 with abrupt changes in isotopic signatures have been reported by Oliveira *et al.* (2016) at IODP
578 Site U1385 (Fig. 6F and 7B) at ca. 390 (U1385-11-fe5), 383 (U1385-11-fe6) and 371.5 ka BP
579 (U1385-11-fe10), interpreted as indicative of the coolest and driest atmospheric conditions
580 of MIS 11. Similar high-intensity forest contractions have also been documented at MD01-
581 2447 around ca. 392, 383 and 375 ka BP (Desprat *et al.*, 2005, 2007), at Lake Ohrid around

582 390 (LO-11-4), 382 (LO-11-5) and 377 ka BP (LO-11-7; Kousis *et al.*, 2018), and at Tenaghi
583 Philippon at 384, 378 and 376 ka BP (Ardenghi *et al.*, 2019). Across all records, the strongest
584 forest contraction appears to be related to the first light-isotopic event 11.24 (event 4 in
585 ODP976 at 397 ka BP) which, as indicated by the marked rise in steppic taxa in our record,
586 appears to be the driest and coolest episode of MIS 11. The other two major forest
587 contractions, synchronous with events 11.23 and 11.22, do not occur alongside a substantial
588 rise in steppic assemblages, indicating that they were predominantly cold events not subject
589 to changes in aridity but still caused a significant strain on temperate oak forests.

590 These high-intensity events have been linked to changes in the AMOC caused by iceberg
591 discharges into the North Atlantic which amplified the cooling process at the end of MIS 11
592 (Oppo *et al.*, 1998; Martrat *et al.*, 2007; Voelker *et al.*, 2010). Concurrent with the three light-
593 isotopic events, Rodrigues *et al.* (2011) show distinctive reductions to ~10°C in their alkenone-
594 based SST record from MD03-2699 (fig. 6E). Similarly, climatic reconstructions from Lake
595 Ohrid show significant drops in MAAT from 8 to 2°C, and reductions in MAP from around 1000
596 to 600mm, demonstrating coeval cooling on land as well as the sea-surface during these
597 events which match the changes in assemblages in our ODP976 record. A parallelism can also
598 be made with the sudden drops in atmospheric CO₂ and CH₄ concentrations and air
599 temperature anomalies from the Antarctic EPICA records (Figs. 6I, J and K) which demonstrate
600 the response of vegetation in the Mediterranean to global-scale climate change.

601 Some authors (Kandiano *et al.*, 2012; Kousis *et al.*, 2018) proposed that drier conditions
602 prevailed in the western Mediterranean and north-western Africa during the millennial-scale
603 climatic events of MIS 11, while wetter conditions occurred in the Balkans, due to the
604 development of a see-saw pattern in precipitation between the western and eastern
605 Mediterranean. While latitudinal and altitudinal differences between sites must be taken into
606 consideration with regard to the climatic reconstructions, abundances of Mediterranean taxa
607 and representation of local/regional pollen signals, this hypothesis may explain the
608 differences in the amplitude of change in vegetation to climate variability observed across the
609 available high-resolution records shown in Figure 7. The changes in forest cover documented
610 in the marine records from ODP976 and U1385, for instance, remain relatively more subdued
611 during both moderate- and high-intensity events compared to Lake Ohrid, where
612 Mediterranean taxa suffer an almost complete disappearance and temperate humid forests
613 undergo much more severe diebacks. At Tenaghi Philippon, high-intensity events seem to
614 impact vegetation at a similar rate to Lake Ohrid, although moderate events do not appear to
615 be as impactful which could be due to the lower altitude of this site (see Tab 1). If the
616 hypothesis that the Balkans were wetter during MIS 11 was correct, this may suggest that
617 vegetation in this region may have reacted more intensely to the impact of cool and especially
618 arid events, while the generally drier conditions in the western Mediterranean and around
619 the Alboran Sea could have benefitted thermophilous vegetation even during harsher
620 climates.

621

622 5.4 Implications for hominin populations

623 Our record from site ODP 976 provides evidence for the strong climatic transition from MIS
624 12 to MIS 11, which undoubtedly influenced hominin populations across Europe. From
625 around 426 ka BP, after the MIS 12 glaciation, modelled population distributions show
626 demographic expansion across Europe (e.g. Blain *et al.* 2021; Rodríguez *et al.*, 2022). The
627 model by Rodríguez *et al.* (2022), for instance, estimates an increase in total population across
628 Western Europe from a range of ~10,000–90,000 individuals during MIS 12a to ~25,000–

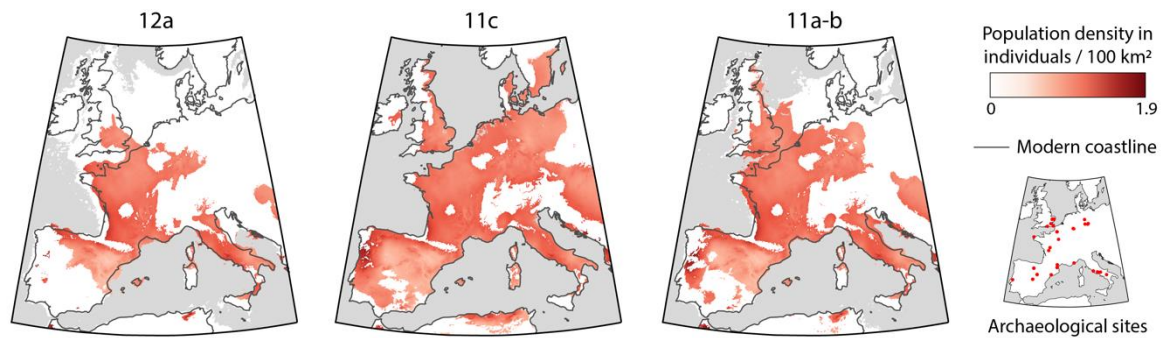


Figure 8 - Density of hominin populations across Western Europe during substages MIS 12a, MIS 11c and MIS 11a-b (adapted from Rodríguez *et al.*, 2022).

629 170,000 individuals during the climatic optimum MIS 11c (Fig. 8). During the transition,
 630 archaeological sites show the emergence of new subsistence behaviours and technical
 631 innovations (core technologies, increase in light-duty tools), and evidence of an early
 632 regionalization of traditions (Moncel *et al.*, 2016, 2020, 2021a,b; García-Medrano *et al.*,
 633 2022a,b). These behavioural changes suggest increased cognition with new skills and social
 634 interactions (Moncel *et al.*, 2015; Peretto *et al.*, 2016). The correspondence of such a
 635 behavioural threshold with the long and stable climatic amelioration observed during the
 636 interglacial MIS 11, especially after the harsh glacial event of MIS 12, leads to the supposition
 637 that climatic amelioration may have led to such social and technological innovations. Such a
 638 long-lasting interglacial period could have encouraged the expansion of favourable territories
 639 for long term occupations of hominins vegetation, fauna and hominin occupation in European
 640 temperate and Mediterranean ecosystems (Berger *et al.*, 2003; Raymo and Mitrovica, 2012;
 641 Oliveira *et al.*, 2016; Moncel *et al.*, 2018; Blain *et al.*, 2021). In particular, the long and stable
 642 climatic optimum of MIS 11c means that hominins would have had a longer time to develop
 643 a deeper level of social networks, better understanding of their direct environment and
 644 potential uses of raw materials, and possibly the spread of the early use of fire (the burning
 645 of fuel in Spain may have only begun after 230 ka BP (Fernández Peris *et al.* 2012), but there
 646 is evidence of charcoal dated to MIS 11 found in fireplaces at Terra Amata in France (Lumley,
 647 2016) and Guado San Nicola in Italy (Lebreton *et al.*, 2019)).

648 The climatic inferences made on the basis of the arboreal expansion in our pollen data
 649 coincide with archaeological finds from Caune de L'Arago in the French Pyrenees, where the
 650 faunal spectrum for MIS 11 was characterised by an assemblage indicative of temperate
 651 conditions, composed of large herbivorous mammals (reindeer, bison, horse and rhinoceros),
 652 carnivores (bears, foxes) and rodents (Barsky *et al.*, 2019). Climatic amelioration during
 653 Termination V would have increased the availability of large herbivores and facilitated the
 654 demographic expansion and mobility of hominins, favouring the diffusion of behavioural
 655 innovations observed during this period.

656 As Szymanek and Julien (2018) and Blain *et al.* (2021) point out, the most favourable
 657 conditions for early hominid settlements comprise a moderately warm and humid climate,
 658 usually during the early or late parts of an interglacial but not during the thermal maximum.
 659 This might suggest that aridity at higher temperatures could have been a limiting factor for
 660 early hominin populations. If, as shown by the comparisons of our pollen data with other
 661 records in the region, the southwestern Mediterranean was generally more arid than central
 662 and eastern Europe, hominins may have preferred to seek areas with greater moisture
 663 availability. This may explain why, in the models by Rodríguez *et al.* (2022) (Fig. 8),

664 southwestern Iberia is less densely populated than other parts of Europe. However, the
665 authors point out that their model is likely to be influenced by the lack of sites with suitable
666 chronologies in this region, limiting our visualisation of the area actually inhabitable by
667 humans (see [Santonja and Pérez-González et al., 2010](#); [Yravedra et al., 2010](#); [Carrión et al.,](#)
668 [2011](#); [Finlayson et al., 2011](#); [Santonja et al., 2014, 2016](#); [Altolaguirre et al 2020](#); [Rubio-Jara et](#)
669 [al., 2016](#); [López-García et al., 2021](#); [Moncel et al., 2021a, b](#); [García-Medrano et al., 2022a](#);
670 [Lockey et al., 2022](#)).

671 [Moncel et al. \(2018\)](#) highlight that the Mediterranean has acted as a refugial area for
672 thermophilous and subtropical taxa throughout the Quaternary. As observed in the ODP976
673 record, vegetation changes in the southwestern Mediterranean were less intense during
674 periods of millennial-scale climatic variability at the end of the MIS 11c optimum and during
675 MIS 11b and 11a. Therefore, it is possible that the persistence of temperate and
676 Mediterranean vegetation in an 'ecological niche' around the Alboran Sea may have
677 facilitated the cultural and technological transition during MIS 11 by providing a reliable
678 source of subsistence. In contrast, during periods of high climatic variability in NW and Central
679 Europe, hominids would have been affected by the contractions of favourable habitats and
680 thereby limited the spread of technological innovations ([Kretzoi and Dobosi 1990](#); [Ashton et](#)
681 [al 2011](#); [Ashton and Davis 2021](#); [Rawlinson et al 2022](#); [Hosfield, 2022](#)).

682 The lack of archaeological sites in this region severely limits our ability to test the validity
683 of this hypothesis, and therefore more work must be undertaken in the southwestern
684 Mediterranean to build a better picture of the spatial distribution of hominins in the
685 southwestern Mediterranean during the MIS 12/11 transition. Improving the coverage of
686 archaeological sites in this region will enable a better understanding of the probability of
687 interactions and interbreeding with other European populations, in turn shedding a light on
688 the role of this region in the development of cultural/technological innovations and the
689 evolution of the Neanderthal lineage.

690

691 **6. Conclusions**

692 This study presented a new high-temporal resolution palynological record from ODP Site 976
693 in the Alboran Sea, which encompasses the MIS 12/11 transition and covers the entirety of
694 MIS 11 until the beginning of MIS 10. Our palynological results provide evidence for the strong
695 climatic shift from glacial to interglacial. The transition from *Pinus*, montane and steppic taxa,
696 to an assemblage comprised of forested temperate and Mediterranean taxa, is coeval with
697 major fluctuations in planktonic records (SST and $\delta^{18}\text{O}$), a sharp increase in Antarctic CO_2 and
698 CH_4 records. The timing of this shift, observed between 430 and 425 ka BP, was correlated
699 with other pollen and marine proxy records from the Mediterranean and North Atlantic,
700 showing a largely synchronous response across the region to global climatic change.

701 A climatic optimum for temperate and Mediterranean taxa is documented between 426
702 and 400 ka BP, which corresponds with the warm substage MIS 11c identified in previous
703 palaeoenvironmental and palaeoclimatic records. The data from ODP976 supports the idea
704 that MIS 11c was an exceptionally prolonged phase, synchronous with maxima in
705 temperature and precipitation, and consistently high greenhouse gas concentrations, likely
706 perpetuated by the unique antiphasing between precession and obliquity that characterised
707 the MIS 11 interglacial.

708 Following the climatic optimum, a slow cooling trend is marked by millennial-scale
709 climatic variability. These events were recognised as moderate-intensity (no counterpart in
710 marine proxies) and high-intensity (signature in marine and terrestrial records). Of the

711 moderate climatic oscillations observed in our record, the most notable was linked to the
712 “Older Holstenian Oscillation” during which a minor forest contraction in temperate forests
713 is observed almost ubiquitously around 408 ka BP across European pollen records. Three high-
714 intensity events were identified at ca. 397, 390 and 378 ka BP and were correlated, keeping
715 chronological uncertainties in consideration, with the light-isotopic events (11.24, 11.23 and
716 11.22) recorded in $\delta^{18}\text{O}$ curves from the Mediterranean and North Atlantic, related to changes
717 in the AMOC. Out of these, possibly the strongest contraction occurred during the insolation
718 minimum at the onset of MIS 11b, which corresponds to the light isotopic event 11.24. The
719 amplitude of the vegetation changes observed at ODP976 during the millennial-scale events
720 may be less intense than what has been previously found in the Balkan Peninsula. This may
721 be due to the overall aridity of the western Mediterranean compared to the east, which could
722 have ensured a prolonged resilience of Mediterranean vegetation during colder conditions.

723 The abrupt shift in vegetation during the MIS12/11 transition and the millennial-scale
724 climatic fluctuations of MIS 11 may be used to infer that hominin populations would have had
725 to adapt to these climatic changes. Climatic amelioration after the harsh glacial of MIS 12 may
726 explain the behavioural threshold observed during the course of the long interglacial MIS 11
727 and internal variations (MIS 11c vs. MIS 11b and 11a). A warmer and wetter climate may have
728 helped the ancestors of the Neanderthal to develop new strategies (subsistence and
729 technological), explaining the population increase and the diffusion of these innovations all
730 over Europe. In the context of the Mediterranean, a generally drier climate during MIS 11
731 compared to central or eastern Europe could have led to a less variable vegetation cover,
732 thereby providing a more reliable source of sustenance during periods of climatic oscillation
733 and thus further facilitating hominin innovations in this period.

734

735 **Acknowledgements**

736 We gratefully acknowledge the financial support of the ANR project Neandroots (Agence
737 Nationale de la Recherche, project N° ANR-19-CE27-0011-01), the Muséum national
738 d’Histoire naturelle (MNHN) and Centre National de la Recherche Scientifique (CNRS). Thanks
739 also to the APLF (Association des Palynologues de Langue Française) for granting funds to
740 participate in the 5th MedPalynoS symposium and present the results of this research
741 internationally. Many thanks also to L. Dubost at the UMR 7194 palynology laboratory for the
742 valuable and efficient technical assistance, and Y. Miras for the support and advice provided
743 during this project. Finally, we thank the Ocean Drilling Program for making the samples
744 available for analysis.

745

746 **References**

747 Alonso, B., Ercilla, G., Martínez-Ruiz, F., Baraza, J., and Galimont, A. (1999). Pliocene-
748 Pleistocene sedimentary facies at Site 976: Depositional history in the northwestern
749 Alboran Sea. *Proceedings of the Ocean Drilling Program: Scientific Results*, 161(1994), 57–
750 68. <https://doi.org/10.2973/odp.proc.sr.161.206.1999>
751 Altolaguirre, Y., Bruch, A.A. and Gibert, L. (2020). A long Early Pleistocene pollen record from
752 Baza Basin (SE Spain): Major contributions to the palaeoclimate and palaeovegetation of
753 Southern Europe. *Quaternary Science Reviews* 231, pp.106199.
754 Ashton, N., & Davis, R. (2021). Cultural mosaics, social structure, and identity: The
755 Acheulean threshold in Europe. *Journal of Human Evolution*, 156, 103011.
756 Ardenghi, N., Mulch, A., Koutsodendris, A., Pross, J., Kahmen, A., and Niedermeyer, E. M.
757 (2019). Temperature and moisture variability in the eastern Mediterranean region during

758 Marine Isotope Stages 11–10 based on biomarker analysis of the Tenaghi Philippon peat
759 deposit. *Quaternary Science Reviews*, 225.
760 <https://doi.org/10.1016/j.quascirev.2019.105977>

761 Azibeiro, L. A., Sierro, F. J., Capotondi, L., Lirer, F., Andersen, N., González-Lanchas, A., Alonso-
762 Garcia, M., Flores, J. A., Cortina, A., Grimalt, J. O., Martrat, B. and Cacho, I. (2021).
763 Meltwater flux from northern ice-sheets to the mediterranean during MIS 12. *Quaternary*
764 *Science Reviews*, 268. <https://doi.org/10.1016/j.quascirev.2021.107108>

765 Barber, D.C., Dyke, A., Hillaire-Marcel, C., Jennings, A.E., Andrews, J.T., Kerwin, M.W.,
766 Bilodeau, G., McNeely, R., Southon, J., Morehead, M.D. and Gagnon, J.M. (1999). Forcing
767 of the cold event of 8,200 years ago by catastrophic drainage of Laurentide
768 lakes. *Nature*, 400(6742), pp.344-348.

769 Barbero, M., Quézel, P., Rivas-Martínez, S., 1981. Contribution á l'étude des groupements
770 forestiers et préforestiers du Maroc. *Phytocoenologia* 9, pp.311–412.

771 Barsky, D., Moigne, A. M., and Pois, V. (2019). The shift from typical Western European Late
772 Acheulian to microproduction in unit 'D' of the late Middle Pleistocene deposits of the
773 Caune de l'Arago (Pyrénées-Orientales, France). *Journal of Human Evolution*, 135.
774 <https://doi.org/10.1016/j.jhevol.2019.102650>

775 Bassinot, F. C., Labeyrie, L. D., Vincent, E., Quidelleur, X., Shackleton, N. J., and Lancelot, Y.
776 (1994). The astronomical theory of climate and the age of the Brunhes-Matuyama mag-
777 netic reversal, *Earth Planet. Sci. Lett.*, 126, pp.91–108

778 Benabib, A. (1982). Bref aperçu sur la zonation altitudinale de la végétation climatique du
779 Maroc, *Ecol. Medit.*, 8(1–2), pp.301–315.

780 Berger, A. (1978). Long-term variations of daily insolation and Quaternary climatic changes.
781 *Journal of Atmospheric Sciences*, 35(12), pp.2362-2367.

782 Berger, A and Loutre, M.F. (1991). Insolation values for the climate of the last 10 million of
783 years. *Quaternary Science Reviews*, 10(4), 297-317.

784 Berger, A. and Loutre M.F. (2003). Climate 400,000 years ago, a key to the future? In: A.W.
785 Droxler, R.Z. *Past Interglacials Working Group of Pages, Interglacials of the last 800,000*
786 *years*. R. of Geop., 54, pp.162-219.

787 Berger, W. H. and Wefer, G. (2003). On the dynamics of the ice ages: Stage-11 paradox, mid-
788 Brunhes climate shift, and 100-ky cycle. *Geophys. Monogr.-Am. Geophys. UNION*, 137,
789 pp.41–60.

790 Blain, H. A., Fagoaga, A., Ruiz-Sánchez, F. J., García-Medrano, P., Ollé, A., and
791 Jiménez-Arenas, J. M. (2021). Coping with arid environments: A critical threshold for
792 human expansion in Europe at the Marine Isotope Stage 12/11 transition? The case of the
793 Iberian Peninsula. *Journal of Human Evolution*, 153.
<https://doi.org/10.1016/j.jhevol.2021.102950>

794 Bout-Roumazeilles, V., Combourieu-Nebout, N., Peyron, O., Cortijo, E., and Masson-Delmotte,
795 V. (2007). Connexion between South Mediterranean climate and North African
796 atmospheric circulation during MIS 3 North Atlantic cold events. *Quaternary Science*
797 *Reviews*, 26, pp.3197–3215.

798 Brandon, M., Landais, A., Duchamp-Alphonse, S., Favre, V., Schmitz, L., Abrial, H., Prié, F.,
799 Extier, T. and Blunier, T. (2020). Exceptionally high biosphere productivity at the beginning
800 of Marine Isotopic Stage 11. *Nature communications*, 11(1), pp.1-10. <https://doi.org/10.1038/s41467-020-15739-2>.

801

802 Brice R. (2007) *Variabilité Climatique en Mer d'Alboran au cours de la Teminaison V (MIS*
803 *12/11)*. Unpublished thesis, University of Bordeaux.

804 Bulian, F., Kouwenhoven, T. J., Jiménez-Espejo, F. J., Krijgsman, W., Andersen, N., and Sierro,
805 F. J. (2022). Impact of the Mediterranean-Atlantic connectivity and the late Miocene
806 carbon shift on deep-sea communities in the Western Alboran Basin. *Palaeogeography,*
807 *Palaeoclimatology, Palaeoecology*, 589. <https://doi.org/10.1016/j.palaeo.2022.110841>

808 Candy, I., Schreve, D. C., Sherriff, J., and Tye, G. J. (2014). Marine Isotope Stage 11:
809 Palaeoclimates, palaeoenvironments and its role as an analogue for the current
810 interglacial. *Earth-Science Reviews*, 128, pp.18–51.
811 <https://doi.org/10.1016/j.earscirev.2013.09.006>

812 Carrión, José S., James Rose, and Chris Stringer. (2011) Early human evolution in the western
813 Palaearctic: ecological scenarios." *Quaternary Science Reviews*, 30(11-12), pp.1281-1295.

814 Chaisson, W. P., Poli, M. S., and Thunell, R. C. (2002). Gulf Stream and Western Boundary
815 Undercurrent variations during MIS 10-12 at site 1056, Blake-Bahama Outer Ridge. *Marine*
816 *Geology*, 189(1–2), pp.79–105. [https://doi.org/10.1016/S0025-3227\(02\)00324-9](https://doi.org/10.1016/S0025-3227(02)00324-9)

817 Combourieu-Nebout, N., Londeix, L., Baudin, F., Turon, J.-L., von Grafenstein, R., and Zahn, R.
818 (1999). Quaternary marine and continental paleoenvironments in the western
819 Mediterranean (Site 976, Alboran Sea): palynological evidence, in: *Proc. ODP Sci. Results*,
820 161: College Station, TX (Ocean Drilling Program), edited by: Zahn, R., Comas, M. C., and
821 Klaus, A., pp.457–468.

822 Combourieu-Nebout, N., Turon, J. L., Zahn, R., Capotondi, L., Londeix, L., and Pahnke, K.
823 (2002). Enhanced aridity and atmospheric high-pressure stability over the western
824 Mediterranean during the North Atlantic cold events of the past 50 k.y. *Geology*, 30(10),
825 pp.863–866. [https://doi.org/10.1130/0091-7613\(2002\)030<0863:EAAHP>2.0.CO;2](https://doi.org/10.1130/0091-7613(2002)030<0863:EAAHP>2.0.CO;2)

826 Combourieu-Nebout, N., Peyron, O., Dormoy, I., Desprat, S., Beaudouin, C., Kotthoff, U., and
827 Marret, F. (2009). Rapid climatic variability in the west Mediterranean during the last
828 25000 years from high resolution pollen data. *Climate of the Past*, 5(3), pp.503–521.
829 <https://doi.org/10.5194/cp-5-503-2009>

830 Dahl, E. (1998). *The Phytogeography of Northern Europe (British Isles, Fennoscandia and*
831 *Adjacent Areas)*. Cambridge Univ. Press, UK.

832 de Kaenel, E., Siesser, W.G., Murat, A. (1999). Pleistocene calcareous nannofossil
833 biostratigraphy and the western Mediterranean sapropels, Sites 974 to 977 and 979. In:
834 Zhan, R., Comas, M.C., Klaus, A. (Eds.), *Proc. ODP Sci. Results.*, 161. College Station, Texas,
835 pp.15–183

836 Desprat, S., Sánchez Goñi, M. F., Turon, J. L., McManus, J. F., Loutre, M. F., Duprat, J., Malaizé,
837 B., Peyron, O., and Peypouquet, J. P. (2005). Is vegetation responsible for glacial inception
838 during periods of muted insolation changes? *Quaternary Science Reviews*, 24(12–13),
839 pp.1361–1374. <https://doi.org/10.1016/j.quascirev.2005.01.005>

840 Desprat, S., Sánchez Goñi, M. F., Naughton, F., Turon, J. L., Duprat, J., Malaizé, B., Cortijo, E.,
841 and Peypouquet, J. P. (2007). Climate variability of the last five isotopic interglacials: Direct
842 land-sea-ice correlation from the multiproxy analysis of North-Western Iberian margin
843 deep-sea cores. *Developments in Quaternary Science*, 7(C), pp.375–386.
844 [https://doi.org/10.1016/S1571-0866\(07\)80050-9](https://doi.org/10.1016/S1571-0866(07)80050-9)

845 Droxler, A. W., Alley, R. B., Howard, W. R., Poore, R. Z., and Burckle, L. H. (2003). Unique and
846 exceptionally long interglacial marine isotope stage 11: Window into earth warm future
847 climate. *Geophysical Monograph Series*, 137(January 2015), pp.1–14.
848 <https://doi.org/10.1029/137GM01>

849 Ellison, C.R.W., Chapman, M.R., Hall, I.R. (2006). Surface and deep ocean interactions during
850 the cold climate event 8200 years ago. *Science* 312, pp.1929–1932.

851 Faegri, F. and Iversen, J. (1989). *Textbook of Pollen Analysis (4th Edition)*. Chichester, UK: John
852 Wiley and Sons.

853 Fernández Peris, J., Barciela González, V., Blasco, R., Cuartero, F., Fluck, H., Sañudo, P. and
854 Verdasco, C. (2012). The earliest evidence of hearths in Southern Europe: the case of
855 Bolomor Cave (Valencia, Spain). *Quaternary International*, 247, pp.267–277.

856 Finlayson, C., Carrión, J., Brown, K., Finlayson, G., Sánchez-Marco, A., Fa, D., Rodríguez-Vidal,
857 J., Fernández, S., Fierro, E., Bernal-Gómez, M. and Giles-Pacheco, F. (2011). The Homo
858 habitat niche: using the avian fossil record to depict ecological characteristics of
859 Palaeolithic Eurasian hominins. *Quaternary Science Reviews*, 30(11-12), pp.1525-1532.

860 Fletcher, W. J. and Sánchez Goñi, M. F. (2008) Orbital- and sub-orbital-scale climate impacts
861 on vegetation of the western Mediterranean basin over the last 48,000 yr. *Quaternary
862 Research*, 70, pp.451–464.

863 Garcia-Gorritz, E., and Garcia-Sanchez, J. (2007). Prediction of sea surface temperatures in the
864 western Mediterranean Sea by neural networks using satellite observations. *Geophysical
865 research letters*, 34(11).

866 García-Medrano, P., Despriée, J., Moncel M-H. (2022a). Innovations in Acheulean biface
867 production at la Noira (Centre France): shift or drift between 700 and 450 ka in Western
868 Europe? *Anthropological and Archaeological Sciences*.

869 García-Medrano, P., Shipton, C., White, M., and Ashton, N. (2022b). Acheulean Diversity in
870 Britain (MIS 15-MIS 11): From the Standardization to the Regionalization of Technology.
871 *Frontiers in Earth Science*, 10, 917207.

872 Girone, A., Maiorano, P., Marino, M., and Kucera, M. (2013). Calcareous plankton response
873 to orbital and millennial-scale climate changes across the Middle Pleistocene in the
874 western Mediterranean. *Palaeogeography, Palaeoclimatology, Palaeoecology*, 392,
875 pp.105–116. <https://doi.org/10.1016/j.palaeo.2013.09.005>

876 González-Donoso, J. M., Serrano, F., and Linares, D. (2000). Sea surface temperature during
877 the Quaternary at ODP Sites 976 and 975 (western Mediterranean). *Palaeogeography,
878 Palaeoclimatology, Palaeoecology*, 162(1–2), pp.17–44. [https://doi.org/10.1016/S0031-
879 0182\(00\)00103-6](https://doi.org/10.1016/S0031-0182(00)00103-6)

880 Hammer, Ø., Harper, D.A. and Ryan, P.D., 2001. PAST: Paleontological statistics software
881 package for education and data analysis. *Palaeontologia electronica*, 4(1), p.9.

882 Hes, G., Goñi, M. F. S., and Bouttes, N. (2022). Impact of terrestrial biosphere on the
883 atmospheric CO₂ concentration across Termination V. *Climate of the Past*, 18(6), pp.1429–
884 1451. <https://doi.org/10.5194/cp-18-1429-2022>

885 Hodell, D. A., Channeil, J. E. T., Curtis, J. H., Romero, O. E., and Röhl, U. (2008). Onset of
886 “Hudson Strait” Heinrich events in the eastern North Atlantic at the end of the middle
887 Pleistocene transition (~640 ka)? *Paleoceanography*, 23(4), pp.1–16.
888 <https://doi.org/10.1029/2008PA001591>

889 Hosfield, R. (2022). Variations by degrees: Western European paleoenvironmental
890 fluctuations across MIS 13–11. *Journal of Human Evolution*, 169, 103213.

891 Hrynowiecka, A., Żarski, M., and Drzewicki, W. (2019). The rank of climatic oscillations during
892 MIS 11c (OHO and YHO) and post-interglacial cooling during MIS 11b and MIS 11a in
893 eastern Poland. *Geological Quarterly*, 63(2), pp.375–394. <https://doi.org/10.7306/gq.1470>

894 Hublin, J. J. (2009). The origin of Neandertals. *Proceedings of the National Academy of
895 Sciences of the United States of America*, 106(38), pp.16022–16027.
896 <https://doi.org/10.1073/pnas.0904119106>

897 Imbrie, J., Hays, J.D., Martinson, D.G., McIntyre, A., Mix, A.C., Morley, J.J., Pisias, N.G., Prell,
898 W.L. and Shackleton, N.J. (1984). The orbital theory of Pleistocene climate: support from a
899 revised chronology of the marine $\delta^{18}\text{O}$ record. In: Berger, A.L., Imbrie, J., Hays, J., Kukla, G.,
900 Saltzman, B. (Eds.), *Milankovitch and Climate*. D. Reidel, Dordrecht, pp. 269–306.

901 Jouzel, J., Masson-Delmotte, V., Cattani, O., Dreyfus, G., Falourd, S., Hoffmann, G., Minster,
902 B., Nouet, J., Barnola, J.M., Chappellaz, J., Fischer, H., Gallet, J.C., Johnsen, S., Leuenberger,
903 M., Loulergue, L., Luethi, D., Oerter, H., Parrenin, F., Raisbeck, G., Raynaud, D., Schilt, A.,
904 Schwander, J., Selmo, E., Souchez, R., Spahni, R., Stauffer, B., Steffensen, J.P., Stenni, B.,
905 Stocker, T.F., Tison, J.L., Werner, M., Wolff, E.W., 2007. Orbital and millennial Antarctic
906 climate variability over the past 800,000 years. *Science*

907 Juggins, S. (2020). *Package "rioja" – Analysis of Quaternary Science Data, The Comprehensive*
908 *R Archive Network*.

909 Kandiano, E.S., Bauch, H.A., Fahl, K., Helmke, J.P., Röhl, U., Pérez-Folgado, M., Cacho, I. (2012).
910 The meridional temperature gradient in the eastern North Atlantic during MIS 11 and its
911 link to the ocean–atmosphere system. *Palaeogeogr., Palaeoclimatol., Palaeoecol.* 333,
912 pp.24–39.

913 Kelly, M.R. (1964). The Middle Pleistocene of North Birmingham. *Philos. Trans. R. Soc. Lond.*,
914 B247, pp.533–592.

915 Kousis, I., Koutsodendris, A., Peyron, O., Leicher, N., Francke, A., Wagner, B., Giaccio, B.,
916 Knipping, M., and Pross, J. (2018). Centennial-scale vegetation dynamics and climate
917 variability in SE Europe during Marine Isotope Stage 11 based on a pollen record from Lake
918 Ohrid. *Quaternary Science Reviews*, 190, pp.20–38.
919 <https://doi.org/10.1016/j.quascirev.2018.04.014>

920 Koutsodendris, A., Müller, U.C., Pross, J., Brauer, A., Kotthoff, U., Lotter, A.F. (2010). Veg-
921 etation dynamics and climate variability during the Holsteinian interglacial based on a
922 pollen record from Dethlingen (northern Germany). *Quaternary Science Reviews* 29,
923 pp.3298–3307

924 Koutsodendris, A., Brauer, A., Pälike, H., Müller, U.C., Dulski, P., Lotter, A.F., Pross, J. (2011).
925 Sub-decadal to decadal-scale climate cyclicity during the Holsteinian interglacial (MIS 11)
926 evidenced in annually laminated sediments. *Climate of the Past*, 7, pp.987–999.

927 Koutsodendris, A., Pross, J., Müller, U. C., Brauer, A., Fletcher, W. J., Kühl, N., Kirilova, E.,
928 Verhagen, F. T. M., Lücke, A., and Lotter, A. F. (2012). A short-term climate oscillation
929 during the Holsteinian interglacial (MIS 11c): An analogy to the 8.2ka climatic event? *Global*
930 *and Planetary Change*, 92–93, pp.224–235.
931 <https://doi.org/10.1016/j.gloplacha.2012.05.011>

932 Koutsodendris, A., Kousis, I., Peyron, O., Wagner, B., and Pross, J. (2019). The Marine Isotope
933 Stage 12 pollen record from Lake Ohrid (SE Europe): Investigating short-term climate
934 change under extreme glacial conditions. *Quaternary Science Reviews*, 221.
935 <https://doi.org/10.1016/j.quascirev.2019.105873>

936 Krtezoi, M. and Dobosi, V.T. (1990). *Vértesszölös Man site and culture*. Akadémiai Kiado,
937 Budapest. 554 p.

938 Kukla, G. (2003). Continental records of MIS 11. *Washington DC American Geophysical Union*
939 *Geophysical Monograph Series*, 137, pp.207-211.

940 Laskar, J., Robutel, P., Joutel, F., tineau, M.G., Correia, A.C.M., Levrard, B., Gastineau, M.,
941 Correia, A.C.M., Levrard, B. (2004). A long-term numerical solution for the insolation
942 quantities of the earth. *AandA* 428, pp.261-285. [https://doi.org/10.1051/0004-](https://doi.org/10.1051/0004-6361:20041335)
943 [6361:20041335](https://doi.org/10.1051/0004-6361:20041335).

944 Lebreton, V., Bertini, A., Russo Ermolli, E., Stirparo, C., Orain, R., Vivarelli, M., Combourieu-
945 Nebout, N., Peretto, C. and Arzarello, M. (2019). Tracing fire in early European prehistory:
946 Microcharcoal quantification in geological and archaeological records from Molise
947 (southern Italy). *Journal of Archaeological Method and Theory*, 26, pp.247-275.

948 Lisiecki, L. E., and Raymo, M. E. (2009). Diachronous benthic $\delta^{18}\text{O}$ responses during late
949 Pleistocene terminations. *Paleoceanography*, 24(3).

950 Lockey, A.L., Rodríguez, L., Martín-Francés, L., Arsuaga, J.L., de Castro, J.M.B, Crété, L.,
951 Martínón-Torres, M., Parfitt, S., Pope, M. and Stringer, C. (2022). Comparing the
952 Boxgrove and Atapuerca (Sima de los Huesos) human fossils: Do they represent distinct
953 paleodemes? *Journal of Human Evolution* 172, 103253.

954 López-García, Juan Manuel, Gloria Cuenca-Bescós, María Ángeles Galindo-Pellicena, Elisa
955 Luzi, Claudio Berto, Loïc Lebreton, and Emmanuel Desclaux. "Rodents as indicators of the
956 climatic conditions during the Middle Pleistocene in the southwestern Mediterranean
957 region: implications for the environment in which hominins lived." *Journal of Human*
958 *Evolution* 150 (2021): 102911.

959 Loulergue, L., Schilt, A., Spahni, R., Masson-Delmotte, V., Blunier, T., Lemieux, B., Barnola,
960 J.M., Raynaud, D., Stocker, T.F., Chappellaz, J. (2008). Orbital and millennial-scale features
961 of atmospheric CH_4 over the past 800,000 years. *Nature*, 453, pp.383-386.

962 Lourens, L.J., 2004. Revised tuning of Ocean Drilling Program Site 964 and KC01B
963 (Mediterranean) and implications for the $\delta^{18}\text{O}$, tephra, calcareous nannofossil, and
964 geomagnetic reversal chronologies of the past 1.1 Myr. *Paleoceanography*, 19, pp.1-20.
965 <https://doi.org/10.1029/2003PA000997>.

966 Loutre, M.F., Berger, A. (2003). Marine Isotope Stage 11 as an analogue for the present
967 interglacial. *Glob. Planet. Change*, 36, pp.209-217. [https://doi.org/10.1016/S0921-](https://doi.org/10.1016/S0921-8181(02)00186-8)
968 [8181\(02\)00186-8](https://doi.org/10.1016/S0921-8181(02)00186-8)

969 Lumley de H. (2016). *Terra Amata. Nice, Alpes-Maritime, France. Comportement et mode de*
970 *vie des chasseurs acheuléens de Terra Amata (Tome V)*. CNRS Editions.

971 Magri, D. and Parra, I. (2002). Late Quaternary western Mediterranean pollen records and
972 African winds. *Earth Planet. Sc. Lett.*, 200, 401–408.

973 Mangili, C., Brauer, A., Plessen, B., Moscariello, A. (2007). Centennial-scale oscillations in
974 oxygen and carbon isotopes of endogenic calcite from a 15,000 varve year record of the
975 Pianico interglacial. *Quat. Sci. Rev.*, 26, pp.1725–1735.

976 Marino, M., Maiorano, P., Tarantino, F., Voelker, A., Capotondi, L., Girone, A., Lirer, F., Flores,
977 J. A., and Naafs, B. D. A. (2014). Coccolithophores as proxy of seawater changes at orbital-
978 to-millennial scale during middle Pleistocene Marine Isotope Stages 14-9 in North Atlantic
979 core MD01-2446. *Paleoceanography*, 29(6), pp.518–532.
980 <https://doi.org/10.1002/2013PA002574>

981 Marino, M., Girone, A., Maiorano, P., Di Renzo, R., Piscitelli, A., and Flores, J. A. (2018).
982 Calcareous plankton and the mid-Brunhes climate variability in the Alboran Sea (ODP Site
983 977). *Palaeogeography, Palaeoclimatology, Palaeoecology*, 508, pp.91–106.
984 <https://doi.org/10.1016/j.palaeo.2018.07.023>

985 Martrat, B., Grimalt, J.O., Shackleton, N.J., de Abreu, L., Hutterli, M.A., Stocker, T.F. (2007).
986 Four climate cycles of recurring deep and surface water destabilizations on the Iberian
987 margin. *Science.*, 317(5837), pp.502-507. doi: 10.1126/science.1139994.

988 McManus, J.F., Oppo, D.W., Cullen, J.L. (1999). A 0.5 million-year record of millennial-scale
989 climate variability in the North Atlantic. *Science* 283, pp.971–975.

- 990 McManus, J.F., Oppo, D.W., Cullen, J.L. and Healey, S. (2003). Marine isotope stage 11 (MIS
991 11): analog for Holocene and future Climate? *Washington DC American Geophysical Union*
992 *Geophysical Monograph Series*, 137, pp.69-85.
- 993 Moncel, M.H., Ashton, N., Lamotte, A., Tuffreau, A., Cliquet, D. and Despriée, J. (2015). The
994 early Acheulian of north-western Europe. *Journal of Anthropological Archaeology*, 40,
995 pp.302-331.
- 996 Moncel, M. H., Arzarello, M., and Peretto, C. (2016). The Holsiteinian period in Europe (MIS
997 11-9). *Quaternary International*, 409, pp.1-8.
998 <https://doi.org/10.1016/j.quaint.2016.06.006>
- 999 Moncel, M. H., Landais, A., Lebreton, V., Combourieu-Nebout, N., Nomade, S., and Bazin, L.
1000 (2018). Linking environmental changes with human occupations between 900 and 400 ka
1001 in Western Europe. *Quaternary International*, 480, pp.78-94.
1002 <https://doi.org/10.1016/j.quaint.2016.09.065>
- 1003 Moncel M-H., Biddittu I., Manzi G., Saracino B., Pereira A., Nomade S., Hertler C., Voinchet P.,
1004 Bahain J-J. (2020) Emergence of regional cultural traditions during the Lower Paleolithic:
1005 evidence of a network of sites at the MIS 11-10 transition in Central Italy (Frosinone-
1006 Ceprano basin). *Anthropological and archaeological sciences*, 12(8), pp.1-32.
- 1007 Moncel M-H., García-Medrano, P., Despriée, J., Arnaud, J., Voinchet, P., Bahain J-J. (2021a).
1008 Tracking behavioral persistence and innovations during the Middle Pleistocene in Western
1009 Europe. Shift in occupations between 700 ka and 450 ka at la Noira site (Centre, France).
1010 *Journal of Human Evolution*. Humans in transition special issue 156, 103009.
1011 <https://doi.org/10.1016/j.jhevol.2021.103009>
- 1012 Moncel M-H., Ashton N., Arzarello M., Fontana F., Lamotte A., Scott B., Muttillio B., Berruti B.,
1013 Nenzioni G., Tuffreau A., Peretto C. (2021b). An Early Levallois core technology between
1014 MIS 12 and 9 in Western Europe? *Journal of Human Evolution*, 139, 102735.
- 1015 Nehrbass-Ahles, C., Shin, J., Schmitt, J., Bereiter, B., Joos, F., Schilt, A., Schmidely, L., Silva, L.,
1016 Teste, G., Grilli, R. and Chappellaz, J., (2020). Abrupt CO₂ release to the atmosphere under
1017 glacial and early interglacial climate conditions. *Science*, 369(6506), pp.1000-1005.
- 1018 Okuda, M., Yasuda, Y., Setoguchi, T. (2001). Middle to late Pleistocene vegetation history and
1019 climatic changes at Lake Kopais, southeast Greece. *Boreas*, 30, 73-82.
- 1020 Oliveira, D., Desprat, S., Rodrigues, T., Naughton, F., Hodell, D., Trigo, R., Rufino, M., Lopes,
1021 C., Abrantes, F., and Sánchez Goñi, M. F. (2016). The complexity of millennial-scale
1022 variability in southwestern Europe during MIS 11. *Quaternary Research* (United States),
1023 86(3), pp.373-387. <https://doi.org/10.1016/j.yqres.2016.09.002>
- 1024 Olson, S.L., Hearty, P.J.A. (2009). A sustained 121m sea level highstand during MIS 11 (400
1025 ka): direct fossil and sedimentary evidence from Bermuda. *Quat. Sci. Rev.* 28, pp.271-285.
- 1026 Oppo, D.W., McManus, J., Cullen, J.C. (1998). Abrupt climate change events 500,000 to
1027 340,000 years ago: evidence from subpolar North Atlantic sediments. *Science*, 279, 1335-
1028 1338.
- 1029 Ozenda, P. (1975). Sur les étages de végétation dans les montagnes du bassin méditerranéen.
1030 *Documents de Cartographie Ecologique*, 16, pp.1-32.
- 1031 Parada, M. and Canton, M. (1998). Sea surface temperature variability in Alboran Sea from
1032 satellite data. *International Journal of Remote Sensing*, 19(13), pp.2439-2450.
- 1033 Peretto, C., Arzarello, M., Bahain, J.J., Boulbes, N., Dolo, J.M., Douville, E., Falguères, C., Frank,
1034 N., García, T., Lembo, G., Moigne, A.M., Muttillio, B., Nomade, S., Pereira, A., Rufo, M.A.,
1035 Sala, B., Shao, Q., Thun Hohenstein, U., Tessari, U., Chiara Turrini, M., Vaccaro, C. (2016).

1036 The Middle Pleistocene site of Guado San Nicola (Monteroduni, Central Italy) on the
1037 Lower/Middle Palaeolithic transition. *Quaternary International*, 411, pp.301-315.

1038 Pierre, C., Belanger, P., Saliege, J.F., Urrutiaguer, M.J., Murat, A. (1999). Paleooceanography of
1039 the western Mediterranean during the Pleistocene: oxygen and carbon isotope records at
1040 site 975. In: Zahn, R., Comas, M.C., Klaus, A. (Eds.). *Proceedings of the Ocean Drilling
1041 Program, Scientific Results*, 161. ODP, College Station, Texas, pp.481–488.

1042 Pross, J., Koutsodendris, A., Christanis, K., Fischer, T., Fletcher, W.J., Hardiman, M., Kalaitzidis,
1043 S., Knipping, M., Kotthoff, U., Milner, A.M. (2015). The 1.35-Ma-long terrestrial climate
1044 archive of Tenaghi Philippon, northeastern Greece: evolution, exploration, and
1045 perspectives for future research. *Newsletters Stratigr.* 48, pp.253-276.

1046 Punt, W., and Blackmore, S. (1991). Oleaceae. *Review of Palaeobotany and Palynology*, 69(1–
1047 3), pp.23–47. <https://doi.org/10.2307/4113622>

1048 Quézel, P. and Médail, F., (2003). *Ecologie et biogéographie des forêts du bassin
1049 méditerranéen*, Elsevier-Lavoisier eds, Paris, France, 571 pp.

1050 Railsback, L.B., Gibbard, P.L., Head, M.J., Voarintsoa, N.R.G., Toucanne, S. (2015). An
1051 optimized scheme of lettered marine isotope substages for the last 1.0 million years, and
1052 the climatostratigraphic nature of isotope stages and substages. *Quat. Sci. Rev.* 111, pp.94-
1053 106. <https://doi.org/10.1016/j.quascirev.2015.01.012>.

1054 Rawlinson, A., Dale, L., Ashton, N., Bridgland, D. and White, M. (2022): Flake tools in the
1055 European Lower Paleolithic: A case study from MIS 9 Britain. *Journal of Human Evolution*
1056 165, 103153.

1057 Raymo, M.E. and Mitrovica, J.X. (2012). Collapse of polar ice sheets during the stage 11
1058 interglacial. *Nature*, 483(7390), pp.453-456.

1059 Regattieri, E., Giaccio, B., Galli, P., Nomade, S., Peronace, E., Messina, P., Sposato, A., Boschi,
1060 C., and Gemelli, M. (2016). A multi-proxy record of MIS 11-12 deglaciation and glacial MIS
1061 12 instability from the Sulmona basin (central Italy). *Quaternary Science Reviews*, 132,
1062 pp.129–145. <https://doi.org/10.1016/j.quascirev.2015.11.015>

1063 Reille, M., de Beaulieu, J.-L. (1990). Pollen analysis of a long Upper Pleistocene continental
1064 sequence in a Velay maar (Massif Central, France). *Palaeogeography Palaeoclimatology
1065 Palaeoecology*, 80, pp.35–48.

1066 Reille, M., and de Beaulieu, J. L. (1995). Long Pleistocene pollen records from the Praclaux
1067 crater, south-central France. *Quaternary Research*, 44(2), pp. 205–215.
1068 <https://doi.org/10.1006/qres.1995.1065>

1069 Reille, M., Andrieu, V., de Beaulieu, J.-L., Guenet, P., Goeury, C. (1998). A long pollen record
1070 from Lac du Bouchet, Massif Central, France for the period 325 to 100 ka (OIS 9c to OIS
1071 5e). *Quaternary Science Reviews*, 17, pp.1107–1123.

1072 Rivas-Martínez, S. (1982). Bioclimatic stages, chorological sectors and series of vegetation in
1073 Mediterranean Spain. *Ecologia mediterranea* , 8(1), pp.275-288.

1074 Rodrigues, T., Voelker, A. H. L., Grimalt, J. O., Abrantes, F., and Naughton, F. (2011). Iberian
1075 Margin sea surface temperature during MIS 15 to 9 (580-300 ka): Glacial suborbital
1076 variability versus interglacial stability. *Paleoceanography*, 26(1), pp.1–16.
1077 <https://doi.org/10.1029/2010PA001927>

1078 Rodríguez, J., Burjachs, F., Cuenca-Bescós, G., García, N., Van der Made, J., González, A.P.,
1079 Blain, H.A., Expósito, I., López-García, J.M., Antón, M.G. and Allué, E. (2011). One million
1080 years of cultural evolution in a stable environment at Atapuerca (Burgos, Spain).
1081 *Quaternary Science Reviews*, 30(11-12), pp.1396-1412.

- 1082 Rodríguez, J., Willmes, C., Sommer, C., & Mateos, A. (2022). Sustainable human population
1083 density in Western Europe between 560.000 and 360.000 years ago. *Scientific Reports*,
1084 12(1), pp.6907.
- 1085 Rubio-Jara, S., Panera, J., Rodríguez-de-Tembleque, J., Santonja, M. and Pérez-González, A.
1086 (2016.) Large flake Acheulean in the middle of Tagus basin (Spain): Middle stretch of the
1087 river Tagus valley and lower stretches of the rivers Jarama and Manzanares valleys.
1088 *Quaternary international*, 411, pp.349-366.
- 1089 Sadori, L., Koutsodendris, A., Panagiotopoulos, K., Masi, A., Bertini, A., Combourieu-Nebout,
1090 N., Francke, A., Kouli, K., Joannin, S., Mercuri, A.M. and Peyron, O. (2016). Pollen-based
1091 paleoenvironmental and paleoclimatic change at Lake Ohrid (south-eastern Europe) during
1092 the past 500 ka. *Biogeosciences*, 13(5), pp.1423-1437.
- 1093 San-Miguel-Ayanz, J., de Rigo, D., Caudullo, G., Houston Durrant, T., Mauri, A. (2016).
1094 *European Atlas of Forest Tree Species*. Publication Office of the European Union,
1095 Luxembourg.
- 1096 Sánchez Goñi, M.F. (2022). *The climatic and environmental context of the Late Pleistocene. In*
1097 *Updating Neanderthals*. Academic Press, pp. 17-38.
- 1098 Sánchez Goñi, M., Eynaud, F., Turon, J. L., and Shackleton, N. J. (1999). High resolution
1099 palynological record off the Iberian margin: direct land-sea correlation for the Last
1100 Interglacial complex. *Earth and Planetary Science Letters*, 171(1), pp.123-137.
- 1101 Sánchez Goñi, M.F., Landais, A., Cacho, I., Duprat, J., Rossignol, L. (2009). Contrasting
1102 intrainterstadial climatic evolution between high and middle North Atlantic latitudes: a
1103 close-up of Greenland interstadials 8 and 12. *Geochemistry, Geophysics, Geosystems*, 10.
1104 <http://dx.doi.org/10.1029/2008GC002369>
- 1105 Sánchez Goñi, M. F., Llave, E., Oliveira, D., Naughton, F., Desprat, S., Ducassou, E., Hodell, D.
1106 A., and Hernández-Molina, F. J. (2016). Climate changes in southwestern Iberia and
1107 Mediterranean Outflow variations during two contrasting cycles of the last 1 Myrs: MIS 31-
1108 MIS 30 and MIS 12-MIS 11. *Global and Planetary Change*, 136, pp.18–29.
1109 <https://doi.org/10.1016/j.gloplacha.2015.11.006>
- 1110 Santonja, M. and Pérez-González, A. (2010). Mid-pleistocene acheulean industrial complex
1111 in the Iberian Peninsula." *Quaternary International* 223, pp.154-161.
- 1112 Santonja, M., Pérez-González, A., Domínguez-Rodrigo, M., Panera, J., Rubio-Jara, S., Sesé, C.,
1113 Soto, E., Arnold, L.J., Duval, M., Demuro, M. and Ortiz, J.E. (2014). The Middle Paleolithic
1114 site of Cuesta de la Bajada (Teruel, Spain): a perspective on the Acheulean and Middle
1115 Paleolithic technocomplexes in Europe. *Journal of Archaeological Science*, 49, pp.556-
1116 571.
- 1117 Santonja, M., Pérez-González, A., Panera, J., Rubio-Jara, S., and Méndez-Quintas, E. (2016).
1118 The coexistence of Acheulean and Ancient Middle Palaeolithic techno-complexes in the
1119 Middle Pleistocene of the Iberian Peninsula. *Quaternary International*, 411, pp.367-377.
- 1120 Shipboard Scientific Party, (1996). Site 976. In: Comas, M.C., Zahn, R., Klaus, A., *et al.*, *Proc.*
1121 *ODP, Init. Repts.*, 161: College Station, TX (Ocean Drilling Program), pp.179–297.
- 1122 Suc, J. P. (1984). Origin and evolution of the Mediterranean vegetation and climate in
1123 Europe. *Nature*, 307(5950), pp.429-432.
- 1124 Szymanek, M. and Julien, M.A. (2018). Early and Middle Pleistocene climate-environment
1125 conditions in Central Europe and the hominin settlement record. *Quaternary Science*
1126 *Reviews*, 198, pp.56-75.

1127 Toucanne, S., Zaragosi, S., Bourillet, J.F., Gibbard, P.L., Eynaud, F., Giraudeau, J., Turon, J.-L.,
1128 Cremer, M., Cortijo, E., Martínez, P., Rossignol, L. (2009). A 1.2 Ma record of glaciation and
1129 fluvial discharge from the West European Atlantic margin. *Q. Sci. Rev.* 28, pp.2974–2981
1130 Turner, C. (1970). The middle Pleistocene deposits at marks Tey, Essex. *Phil. Trans. R. Soc. B.*,
1131 257, pp.373-437.

1132 Tye, J., Sherriff, J., Candy, I., Coxon, P., Palmer, A., McClymont, E.L. and Schreve, D.C. (2016).
1133 The $\delta^{18}\text{O}$ stratigraphy of the Hoxnian lacustrine sequence at Marks Tey, Essex, UK:
1134 implications for the climatic structure of MIS 11 in Britain. *Journal of Quaternary Science*,
1135 31(2), pp.75-92.

1136 Tzedakis, P.C. (1993). Long-term tree populations in northwest Greece through multiple
1137 Quaternary climatic cycles. *Nature*, 364, pp.437–440.

1138 Tzedakis, P.C. (1994). Vegetation change through glacial-interglacial cycles: a long pollen
1139 sequence perspective. *Philosophical Transactions Royal Society London*, B 345, pp.403–432

1140 Tzedakis, P. C., Andrieu, V., de Beaulieu, J. L., Crowhurst, S., Follieri, M., Hooghiemstra, H.,
1141 Magri, D., Reille, M., Sadori, L., Shackleton, N. J., and Wijmstra, T. A. (1997). Comparison
1142 of terrestrial and marine records of changing climate of the last 500,000 years. *Earth*
1143 *Planet. Sci. Lett.*, 150, pp.171–176.

1144 Tzedakis, P. C., Andrieu, V., de Beaulieu, J. L., Birks, H. J. B., Crowhurst, S., Follieri, M.,
1145 Hooghiemstra, H., Magri, D., Reille, M., Sadori, L., Shackleton, N. J., and Wijmstra, T. A.
1146 (2001). Establishing a terrestrial chronological framework as a basis for biostratigraphical
1147 comparisons. *Quaternary Science Reviews*, 20(16–17), pp.1583–1592.
1148 [https://doi.org/10.1016/S0277-3791\(01\)00025-7](https://doi.org/10.1016/S0277-3791(01)00025-7).

1149 Tzedakis, P. C., Hooghiemstra, H., and Pälike, H. (2006). The last 1.35 million years at Tenaghi
1150 Philippon: revised chronostratigraphy and long-term vegetation trends. *Quaternary*
1151 *Science Reviews*, 25(23–24), pp.3416–3430.
1152 <https://doi.org/10.1016/j.quascirev.2006.09.002>

1153 Tzedakis, P. C., Pälike, H., Roucoux, K. H., and de Abreu, L. (2009). Atmospheric methane,
1154 southern European vegetation and low-mid latitude links on orbital and millennial
1155 timescales. *Earth Planet. Sci. Lett.*, 277, pp.307–317

1156 Tzedakis, P. C., Hodell, D. A., Nehrbass-Ahles, C., Mitsui, T., and Wolff, E. W. (2022). Marine
1157 Isotope Stage 11c: An unusual interglacial. *Quaternary Science Reviews*, 284, 107493.
1158 <https://doi.org/10.1016/j.quascirev.2022.107493>

1159 Vakhrameeva, P., Koutsodendris, A., Wulf, S., Fletcher, W. J., Appelt, O., Knipping, M.,
1160 Gertisser, R., Trieloff, M., and Pross, J. (2018). The cryptotephra record of the Marine
1161 Isotope Stage 12 to 10 interval (460–335 ka) at Tenaghi Philippon, Greece: Exploring
1162 chronological markers for the Middle Pleistocene of the Mediterranean region. *Quaternary*
1163 *Science Reviews*, 200, pp.313–333. <https://doi.org/10.1016/j.quascirev.2018.09.019>

1164 Vázquez Riveiros, N., Waelbroeck, C., Skinner, L., Duplessy, J. C., McManus, J. F., Kandiano, E.
1165 S., and Bauch, H. A. (2013). The “MIS 11 paradox” and ocean circulation: Role of millennial
1166 scale events. *Earth and Planetary Science Letters*, 371–372, pp.258–268.
1167 <https://doi.org/10.1016/j.epsl.2013.03.036>

1168 Voelker, A. H. L., Rodrigues, T., Billups, K., Oppo, D., McManus, J., Stein, R., Hefter, J., and
1169 Grimalt, J. O. (2010). Variations in mid-latitude North Atlantic surface water properties
1170 during the mid-Brunhes (MIS 9-14) and their implications for the thermohaline circulation.
1171 *Climate of the Past*, 6(4), pp.531–552. <https://doi.org/10.5194/cp-6-531-2010>

1172 von Grafenstein, U, Erlenkeuser, H., Brauer, A., Jouzel, J. and Johnsen, S.J. (1999). A mid-
1173 European decadal isotope-climate record from 15,500 to 5000 years
1174 BP. *Science*, 284(5420), pp.1654-1657.

1175 Wagner, B., Vogel, H., Francke, A., Friedrich, T., Donders, T., Lacey, J.H., Leng, M.J., Regattieri,
1176 E., Sadori, L., Wilke, T. and Zanchetta, G. (2019). Mediterranean winter rainfall in phase
1177 with African monsoons during the past 1.36 million years. *Nature*, 573(7773), pp.256-260.

1178 West, R.G. (1956). The Quaternary deposits of Hoxne, Suffolk. *Philosophical Transactions of*
1179 *the Royal Society of London, Series, B* 239, pp.265–356.

1180 Wijmstra, T.A., Smit, A. (1976). Palynology of the middle part (30 to 78m) of the 120m deep
1181 section in Northern Greece (Macedonia). *Acta Botanica Neerlandica* 25, pp.297–312.

1182 Yravedra, J., Domínguez-Rodrigo, M., Santonja, M., Pérez-González, A., Panera, J., Rubio-Jara,
1183 S. and Baquedano E. (2010). Cut marks on the Middle Pleistocene elephant carcass of
1184 Áridos 2 (Madrid, Spain). *Journal of Archaeological Science*, 37(10), pp.2469-2476.

1185

1186